

ANSWERS TO REFEREE#1

1) While the first half of the manuscript is well-structured, the second half is not. I would strongly recommend combining Results and Discussion sections or providing a clear separation between these sections with regard to contents. A major part of the actual results (including several figures) is introduced in the Discussion section, partially in fact without much discussion, context or explanation. This is not what a reader of this article would expect.

ANSWER: the authors feel that to the contrary, figures presented in the Discussion section are not straightforward representations of experimental results but rather either statistical / analytical modeling results (i.e. $\delta^2\text{H}$ - $\delta^{18}\text{O}$ relationships / δS gradients dynamics). This is why the authors would like to keep Results / Discussion as separate sections.

2) The readability of the manuscript would clearly benefit from revising for sentence structure and grammar (e.g., avoid frequent use of very long sentences, use proper punctuation).

ANSWER: effort has been made in the revised text to reformulate and significantly shorten sentences containing more than 30 words.

3) It is not clear how the method described in the paper is new (Abstract P3894LL8; Conclusions P3906LL19). In the manuscript text (e.g. P3896), it is stated that a previously developed method is applied directly. As such, the declaration of methodological novelty seems inappropriate.

ANSWER: the present study is the first application of the method of Rothfuss et al. (2013) which provided the calibration coefficients for ^2H and ^{18}O and (Eq. 1 and 2) solely. This study is also the very first long-term application of the series of newly developed similar monitoring systems based on gas-permeable membranes (i.e., Herbstritt et al., 2012; Volkmann and Weiler, 2014). This has been clearly stated in the revised text (i.e., in Abstract, Material and Methods and in Conclusion).

4) It is not entirely clear how to interpret the ambient/atmospheric air measurements. Apparently, one measurement location was maintained in a room with a small soil column while an AC circulated air with unknown isotopic composition. It seems that the influence of air supplied by the AC on the vapor mixture that is assessed here would likely vary over time, but this issue does not become very clear. For example, P3904LL12/P3905LL2, why was the deuterium abundance that high and why was there no dO-dD correlation then? Temperature is implicitly suggested as a relevant covariate, but no clear explanation is provided. It should generally be explained what the informative value and validity of atmospheric data collected during the experiment is.

ANSWER: through the significant statistical link between air temperature and atmosphere isotope compositions, it is inferred in the text that the laboratory air moisture partly originated from outside air moisture. However, as air temperature seasonal dynamics could not alone explain that of the atmosphere isotope compositions, it is also concluded that laboratory air moisture was impacted by column water evaporation. The fact that the atmospheric $\delta^2\text{H}$ values measured during the experimental period DoE 125-155 were remarkably high is directly related to the high soil $\delta^2\text{H}_{\text{liq}}$ values during that same period (see Figure 4d). The reviewer is right, this need to be explicitly written and will be in §4.2

Please also note that the AC system did not bring outside air into the laboratory whereas it cooled (without condensation) and re-circulated the laboratory air by the set of axial fans. This has been better explained in the revised text.

5) Throughout section 4.2 (PP3904LL7), significant results, existing and non-existing correlations are reported and further used to support conclusions without suitable statistical inference. I do not believe the conclusions are generally unjustified, but the statistical assessment and report needs to be improved. E.g., I would expect confidence intervals on slope estimates, and appropriate tests on difference between slopes.

ANSWER: F-statistics p-values have been given along with R-squared in the revised text. Note that p-values are almost exclusively lower than 0.001 apart from some regressions having $p < 0.01$.

Further (P3904L18), a (presumably) OLS regression using data from all soil depths (with expectedly differing slope) does not seem appropriate (regarding residual structure) or useful (a consistent slope would not be expected).

ANSWER: The authors agree with this remark. However this is typically what an experimentalist would do to check the extent of bare soil evaporation: plot $\delta^{18}O$ against δ^2H for entire soil profiles. The vertical resolution of our method was high enough to allow visualizing these significantly different $\delta^2H_{liq}-\delta^{18}O_{liq}$ LRS in 01-03-05 cm depth. And this is why the authors finally differentiate these surface data from the rest of the soil profiles. Note that p-values of all estimated regression parameters (slope/y-intercept) are lower than 0.001.

Also, R-squared is the coefficient of determination (not correlation; e.g. Fig. 6). Finally, negative coefficients of determination cannot be found (P3905L4) and negative slopes do not point to lack of linear relation.

ANSWER: Thank you for these corrections. There was indeed a typographical error: only $\delta^2H_a-\delta^{18}O_a$ regression slope is negative whereas R-squared equals 0.26 (p -value < 0.001). This has been corrected in the revised text along with “determination” instead of “correlation” in Fig. 6.

6) It is not clear if δS_{vap} is calibrated to the reference scale. The contrary seems to be the case from p3899. In that case the values would, however, not be comparable (e.g. P3901LL15) with equilibrium vapor compositions of a known liquid water on the reference scale.

ANSWER: indeed, this was not clear in the text. This following sentence:

“ δ_a and δ_S values were finally corrected for laser instrument drift with time, using the isotope compositions of the two water standards, δ_{st1} and δ_{st2} .”

has been reformulated as:

“ δ_a , $\delta_{S_{vap}}$ and δ_S values were finally corrected for laser instrument drift with time, using the isotope compositions of the two water standards, δ_{st1} and δ_{st2} .”

Minor comments:

P3896L18: "Average" should be plural and also more specific, presumably "Mean values".

ANSWER: thank you for this proposition. This has been adopted in the revised version.

P3897L20: Consider using, e.g., δS_{liq} rather than δS . The use of δS and δS_{vap} is somewhat confusing. Also, the latter seems to refer to partially corrected values, this could be made clearer.

ANSWER: δ_S has been replaced with $\delta_{S_{liq}}$ throughout the manuscript in the revised text, the equations, and the figure captions.

P3899L7: Are the SDs mean or maximum values across samples?

ANSWER: the reported SDs are the maximal accepted standard deviations values. This has been specified in the revised text as such:

“Measurements that did not fulfil the above mentioned conditions for $\delta^2\text{H}$ and $\delta^{18}\text{O}$ standard deviations were not taken into account”

P3899LL26: It is not clear which experimental measure was used here to achieve the declared goal.

ANSWER: the method with which water was applied to the sand surface has been further described by adding the following sentence:

“Opening/closing the valve controlled the flow rate at which air entered the bottle headspace, which in turn controlled the irrigation flow rate.”

PP3904LL12: A brief comment on some of the underlying concept (e.g. kinetics) leading to the stated conclusion could be helpful for interested non-expert readers.

ANSWER: Concepts on isotopic kinetic effects has been given in the revised text. The last sentence of 4.2 2nd §, i.e.,

“Therefore, it can be deduced that the laboratory air moisture was partly resulting from column evaporation.”

has been replaced with:

“ $\delta^2\text{H}$ - $\delta^{18}\text{O}$ regression slope typically lower than eight indicate that a water body has been affected by (non-equilibrium) evaporation process. A good approximation for the slope of the ‘evaporation line’ given by Gat (1971) (Eq. (3), based on the Craig and Gordon (1965) model) depends in addition on the aerodynamic conditions at the liquid/air interface, i.e., relative humidity and the so-called kinetic fractionation factor (Merlivat, 1978 ; Cappa et al., 2003; Luz et al., 2009). Therefore, it can be deduced that the laboratory air moisture was partly resulting from column evaporation.”

P3904LL13: The reference used for inference of equilibration fractionation factors should be given.

ANSWER: the reference (Majoube, 1971) has been added to the revised version:

“Majoube, M.: Oxygen-18 and Deuterium Fractionation between Water and Steam, J. Chim. Phys. Phys.-Chim. Biol., 68, 1423-1436, 1971.”

ANSWERS TO REFEREE#2

The paper has two flaws in my opinion: 1. there is almost no discussion, only results and 2. it is overselling evidence for prove.

I-1) Regarding point 1: This is such nice data so I am really missing the discussion. For example, it is reported that the upper soil layers exhibit different lines in d18O-dD space.

But no explanation is given why. There are already no meteoric water lines in the plots to compare.

ANSWER: meteoric water lines will be incorporated in the plots

I-2) What would you expect if you think about evaporation lines? Gat has shown that the observed evaporation line is a combination of several evaporation lines at different temperatures. Could you do something similar?

I-3) I think that figure 7 does not add anything to the manuscript.

I-4) Another point of discussion could be the value of the kinetic fractionation factor. One has E and VPD so one gets the conductance. One has also theta at the soil surface and the atmospheric conditions. So you can estimate the enrichment at the evaporating front and hence can deduce the equilibrium fractionation that fits best. Are Mathieu and Bariac right, what seems to be suggested by recent studies? Or is it completely wrong because it neglects the resistance in the soil for the evaporation? I guess evaporation E was deduced from the change of the soil moisture profile. This was not explained in the manuscript. So if you can do that, can you then also get the isotopic composition of the evaporation from the change in the isotope profile?

And if so, what for do I need the evaporating front?

ANSWER: The reviewer is right that the data could be further discussed to retrieve information on kinetic fractionation factors. In the revised version of the manuscript, we show that simulated values of evaporation line slopes obtained for 10 consecutive days of isotopic data and using the expression proposed by Gat (1971, #1) (based on the Craig and Gordon model, 1965 #2) lead to a good estimation of the measured slopes ($R^2 = 0.76$; $p < 0.001$). For this kinetic fractionation factors were computed using vapor diffusivities ratios from Merlivat (1978, #3) and n exponent from Mathieu and Bariac (1996, #4). Surface soil moisture was calculated from data above the evaporation front whereas the isotope compositions in the liquid phase at the evaporation front as estimated in §4.3.

Determining the evaporation isotope composition from changes in the isotope profile is a great idea which unfortunately cannot be validated here as we do not measure the evaporation isotope compositions. Nevertheless in the revised manuscript, the authors will provide time series of evaporation isotope compositions calculated using Craig and Gordon model with Mathieu and Bariac formulations for n exponent.

Note that evaporation rate was deduced from changes in mass measured by a weighing balance (P3898L20-21).

Finally, the authors would like to keep Figure 7 as it illustrates with a dual-isotope approach the increasing link between atmosphere and soil surface water vapors.

#1 Gat, J.: Comments on the Stable Isotope Method in Regional Groundwater Investigations, Water Resour. Res., DOI: 10.1029/WR007i004p00980, 1971

#2 Craig, H., and Gordon, L. I.: Deuterium and oxygen 18 variations in the ocean and marine atmosphere, Stable Isotopes in Oceanographic Studies and Paleotemperatures, Spoleto, Italy, 1965, 9-130, 1965.

#3 Merlivat, L.: *Molecular Diffusivities of H₂16O, HD16O, and H₂18O in Gases*, *J Chem Phys*, DOI: 10.1063/1.436884, 1978

#4 Mathieu, R., and Bariac, T.: *A numerical model for the simulation of stable isotope profiles in drying soils*, *J Geophys Res-Atmos*, DOI: 10.1029/96jd00223, 1996

I-3) I was also wondering if you can deduce soil moisture from the humidity in the tubes? I could not find a word about it in Rothfuss et al. (2013) but some sentence in this manuscript made me think that it should be possible.

ANSWER: It could be theoretically feasible from mass balance calculations. However one would need the soil water vapor output flow rate value, which was not measured. Only input flow rate was set which could differ, especially under dry conditions, with soil water vapor output flow rate.

II-1) Regarding point 2: The study is an application of the method developed earlier and presented in Rothfuss et al. (2013). But the abstract states: "In this study, we present a new non-destructive method ..." The enrichment at the evaporating front is well known, often observed and explained at least since Barnes and Allison (1984). But the abstract states: "we could also show for the first time the increasing influence of the isotopically depleted ambient water vapour on the isotopically enriched liquid water close to the soil surface (i.e., atmospheric invasion)."

ANSWER: This is true that Barnes and Allison (1983a, 1983b, and 1984) measured and modelled the depth of the evaporation front, however at permanent and isotopic steady states. Their measured isotopic profiles are unique solutions obtained for given and constant atmospheric conditions (as well as with unique values for soil physical properties such as tortuosity). In the present study, we documented for the first time the dynamics of the evaporation front from our isotopic data with a daily temporal resolution. This will be specified as such in the conclusion. Moreover in contrast with e.g., Barnes and Allison studies, the daily estimation of evaporation front is inferred not from the maximum steady state soil water isotope compositions but from maximum isotopic gradients.

II-2) The same in the conclusions. It is stated, for example, "it could capture sudden variations following a simulated intense rain event." It is true that the method reacted to the watering. No attempt was done, though, to quantify if the observed change in isotopes fits to the isotopic water balance.

ANSWER: No attempt was indeed made to quantify if the isotopic water balance corresponded well with the addition of water. However, similarly to our answer to your comment I-4) the isotope composition of Evaporation flux is needed to close this isotopic water balance. This was not available during the experiment.

II-3) Also "followed quantitatively the progressive isotope enrichment" was not proven. The authors took the calibration done in another medium; at least it sounded different to the sand in Rothfuss et al. (2013). I have always wondered about the physics behind the calibration curve. For example, why is the observed offset not the equilibrium fractionation at 0 degC? So to me it was not proven that the same calibration curve is valid for different soils. There could be a dependency of the soil, which was also hinted in section 4.1.

ANSWER: The method was calibrated with pure quartz sand with very similar pore size distribution and density, and with no organic matter. It is true that other natural soils having high

clay and/or salt content(s) might need other calibrations. This is not the case in the present study. Note, that we correct these calibrated readings with those of the two laboratory standards, which account for soil properties as well as aging of the tubings etc. Why Rothfuss et al. (2013) could not simply keep the equilibrium fractionation values measured by Majoube (1971) (or from any other authors for that matter) has to do with how the soil vapor phase is actively sampled.

III-1) I have a few other questions and comments: The method for determining the evaporating front is very flawed. I would have at least fitted some kind of spline to determine the front. Otherwise you are limited to the resolution of your measurements.

But in any case, the evaporating front does not have to be the maximum. This depends on the atmospheric value. It can be even seen in the measurements presented in deuterium on DoE 100-150: The profile is pretty vertical in the upper soil while the front is already a few cm down the soil. It is not the maximum of the curve but rather the point of a discontinuity in the first derivative that indicates the evaporating front.

ANSWER: The gradients were simply calculated using a linear approximation of the composition profiles between two observation depths. We did not use splines because the non-monotonous change of the isotope compositions with depth could lead to considerable uncertainties.

The reviewer makes the correct remark that the depth of the evaporation front does not necessarily corresponds with the depth where the observed isotope compositions are the largest. If the maximum isotope compositions are used to define the depth of the evaporation front, then the invasion of the evaporation front in the porous medium is predicted at later times. Secondly, the two different isotopes then lead to considerable differences in the prediction of the depth of the evaporation front. For Deuterium, the compositions in the upper two observation depths are almost equal to each other for most of the times so that it is hardly possible to derive the evaporation depth from the maximal composition measurement. However, the temporal evolution of the vertical gradients in isotope composition is more consistent for the two isotopes. It can also be argued that below the evaporation front, the gradient is positive and decreases with depth. Above the evaporation front, atmosphere water vapor with lower isotope compositions intrudes in the porous medium. This reduces in a first phase the increase of isotope compositions which results from isotope enrichment at the evaporation front.

Only after a certain time, the intrusion of atmosphere vapor will result in a decrease in isotope compositions above the evaporation front. But, the intrusion of atmosphere water vapor which slows down the increase in compositions has an effect on the vertical isotope composition gradients above the evaporation front: they start to decrease and become smaller than the isotope composition gradients below the evaporation front before the compositions start decreasing with time.

A more in depth investigation of the behavior of the composition gradients with time and depth will be carried out in a follow-up study with detailed numerical simulations using the isotope-enabled SVAT SiSPAT-Isotope.

III-2) Why is there no decrease in water content in the lowest layer. It seems like standing at 0.3x and not moving for 300 days. This is impossible with a porous glass plate at the bottom. And quite contrary to Merz et al. (2014). Did you really have a porous plate on the bottom? If not, this is the reason why you do not see stage I evaporation.

ANSWER: The reason why water content was almost constant for 300 days from -0.3 m depth down to the bottom of the column is explained by the fact that the soil column was sealed directly below the porous glass plate (2-way valve was in closed position, P3898L 19-20).

Nevertheless, even if the 2-way valve was maintained opened during the experiment, the properties of the porous plate would not allow drainage or evaporation of water. The porous

glass plate has an air entry value of 0.87 m (computed from the pore size distribution), which is larger than the maximum possible water column length (i.e., 0.6 m, when soil is saturated at the very beginning of the experiment).

III-3) So there in an argument in section 4.3 that the resistance increases with increased wind speed and this is why there is no stage I evaporation. This is unphysical. The exact opposite is true and also measured very often, even in the same institute.

ANSWER: We meant that the transfer resistance increases with decreasing water content in relative terms more for a thin (high wind velocity) than for a thick (low wind velocity) boundary layer. This does not mean that the transfer resistance for a fully wet surface is higher for a high than for a low wind velocity.

In the revised text, the following § (P3905L11-15):

“This indicates greater wind velocity in the air layer above the soil column due to the laboratory ventilation system which would lead to a decrease in evaporation rate during stage I due to an increased transfer resistance in the boundary layer above the drying porous medium as observed and modelled by Shahraeeni et al. (2012).”

was reformulated as:

“This indicates greater wind velocity in the air layer above the soil column due to the laboratory ventilation. For higher wind velocities, the boundary layer above the drying medium is thinner and the transfer resistance for vapor transfer lower than for lower wind velocities. But, for thinner boundary layers, the evaporation rate depends stronger on the spatial configuration of the vapor field above the partially wet evaporating surface. Evaporation rate decrease (and the transfer resistance in the boundary layer increase) with decreasing surface water content more for higher than for lower wind velocities (Shahraeeni et al., 2012).”

III-4) The discussion about the atmospheric water vapour is strange. What does it mean: "These values were significantly lower than the calculated ratio of the equilibrium fractionation for $1\text{H}2\text{H}16\text{O}$ and $1\text{H}2\text{H}18\text{O}$ that characterises meteoric water bodies, which should have ranged between 8.32 (DoE 200–250) and 8.47 (DoE 0–50) at the measured laboratory air temperatures." Atmospheric air is long-range transport. It has nothing to do with "the measured laboratory air temperatures". Why does it has to be in equilibrium with some meteoric water bodies? What are these bodies? Did you check the weather patterns? Could have been air from the East instead from the West as normal.

ANSWER: Indeed! This is a mistake and this has been corrected in the revised version of the manuscript where instead of laboratory air temperature, local daily mean air temperatures were taken into account for calculating ranges of temperature-dependent meteoric water lines slopes.

III-5) Last but not least, the manuscript uses very often 'isotope' where it should be the adjective 'isotopic' such as in isotopic composition.

ANSWER: Following T.B. Coplen (Guidelines and recommended terms for expression of stable-isotope-ratio and gas-ratio measurement results, RCMS, 2011), both 'isotope' and 'isotopic' apply. When e.g., looking at the reference list of this manuscript, 'isotope' is preferred no less than 10 times over 'isotopic'.

ANSWERS TO CHRISTINE STUMPP, EDITOR

1) The reviewers pointed out that comparison to other studies is missing in the discussion. As no answer was provided by the authors, I want to emphasize that the authors need to address it when revising their manuscript.

ANSWER: The authors now compare their results with those of Barnes and Allison (1988), Brunel et al. (1995), DePaolo et al. (2004), and Braud et al. (2009a and b)

2) I disagree to combine the results and discussion chapter. However, I recommend moving chapter 4.2 into the results chapter. Here, measured data are presented just in a different way and not discussed. Still, an explanation and discussion of the d2H-d18O relationship needs to be included in a revised version of the manuscript.

ANSWER: chapter 4.2 was moved in the Results section (now 3.6)

3) As already indicated in the answers, kinetic fractionation factors will be presented in the revised version. To my opinion, the manuscript would benefit from some theoretical calculations similar to the zero infiltration conditions in Singleton et al. (2004; cited in the manuscript).

ANSWER: theoretical calculations are now provided (Chapter 2.7 and 4.3). The editor is right, our manuscript would certainly gain from numerical simulations results. This is however not the intention of the present manuscript. As written at the end of chapter 4.3, a more in depth investigation of the behavior of evaporation slopes (and isotope composition gradients with depth) with time could be carried out with detailed numerical simulations using an isotope-enabled SVAT model such as SiSPAT-Isotope.

4) As already indicated by the reviewers, the interpretation of the ambient air measurements is highly speculative in the current version of the manuscript. Even though the authors stated that the air condition did not exchange the air in the lab, it is not a closed system. There can be other reason why the slopes are changing (other water sources, opening the door etc.).

ANSWER: you are absolutely right: your comment was inserted in the document (§3.6)

More evidence needs to be provided e.g. by adding some theoretical calculations of evaporation and mixing lines.

ANSWER: calculation of evaporation lines are now provided §4.3

Further, is there a correlation between the atmospheric d-Excess and the evaporation flux? Or the d-Excess of the upper soil layers and evaporation flux? The evaporation is highest at the beginning of your experiment. However, (i) slopes are not impacted here and (ii) the humidity did not change indicating that the contribution of water vapor to the lab atmosphere is negligible.

ANSWER: calculation of d-Excess would be redundant with calculations of evaporation lines' slopes presented in §4.3, plus less insights into the physics of vapor transport through the soil surface layer from the evaporation front would be possible

Minor comments:

Abstract, ln 8-9: the long-term application is new, not the method itself

ANSWER: this is now clearly stated in the abstract

3895, In 20: according to Fick's law

ANSWER: done, thank you

3895, In 24: HYDRUS not Hydrus

ANSWER: done

3896, In 2-3: For water samples, also suction cups are non-destructive methods which have been frequently used (e.g. in combination with lysimeters). However, the great benefit of the study is that you get "continuous" (high temporal resolution) information and high spatial resolution.

ANSWER: Thanks you for this remark. This was added in the text with the precision that suction cups allow for sampling water whose tension is higher than -600 hPa.

3896, In 5: see similar approach of Gaj et al. 2015, HESSD

ANSWER: reference was added.

3897: Did you check the water at the end of your experiment to verify that there were no fractionation effects over time? Are these closed vessels. Even when looking at Rothfuss et al. 2013, I have difficulties to understand your internal standard system.

ANSWER: These are closed vessels (specified in the text). The isotope compositions were not measured after the experiment. However in the study of Rothfuss et al. (2013), vessels were checked for signs of evaporative enrichments after three months of intensive use, fortunately without success (isotope compositions of water pumped out of the vessels were not higher than those of waters used them).

3898, In 7: how was lab air sampled?

ANSWER: laboratory air was sampled passively with a 1/8" three meter-long stainless steel tubing at 2 m above the sand surface. This is now specified in Chapter 2.4.

3898, In 17: in situ (italic)

ANSWER: done

3900, In 16-19: It is actually difficult to see the changes in the raw data of Figure 2

ANSWER: Y-axis of figure 2b has been enlarged to better visualize these differences.

3903, chapter 4.1: the word "very" is often used; this is a rather subjective word and can be deleted (e.g. there is no difference between "very tightly" and "tightly" bound water - as long as you do not use it in a quantitative way).

ANSWER: Indeed, this is too subjective. "very" was erased from the chapter.

3904, In 6: Why not splitting the observation period into the same days like in Figure 5? These three groups represent the three phases of your experiment: (i) evaporation, (ii) water-atmospheric vapor equilibration (iii) irrigation.

ANSWER: The idea behind figure 6 is to compare $\delta^{18}O$ - δ^2H LRS between periods. These periods should be of equal length.

Figure 2: stick to SI units like in the text and report depths in meter (not centimeter)

ANSWER: A new figure 2 has been incorporated into the manuscript, where soil depths are reported in meters.

Figure 4, caption: soil temperature is not shown; delete in caption

ANSWER: indeed (!). This was corrected.

Figure 5: just an idea: is d-Excess giving you any additional information?

ANSWER: please report to our answer to your comment above.

Long-term and high frequency non-destructive monitoring of water stable isotope profiles in an evaporating soil column

Y. Rothfuss¹, S. Merz¹, J. Vanderborght¹, N. Hermes¹, A. Weuthen¹, A. Pohlmeier¹, H. Vereecken¹ and N. Brüggemann¹

[1]{Forschungszentrum Jülich GmbH, Institute of Bio- and Geosciences, Agrosphere Institute (IBG-3), Leo-Brandt-Straße, D-52425 Jülich, Germany}

Correspondence to: Y. Rothfuss (y.rothfuss@fz-juelich.de)

Abstract

The stable isotope compositions of soil water ($\delta^2\text{H}$ and $\delta^{18}\text{O}$) carry important information about the prevailing soil hydrological conditions and for constraining ecosystem water budgets. However, they are highly dynamic, especially during and after precipitation events. The classical method of determining soil water $\delta^2\text{H}$ and $\delta^{18}\text{O}$ at different depths, i.e., soil sampling and cryogenic extraction of the soil water, followed by isotope-ratio mass spectrometer analysis is destructive and laborious with limited temporal resolution. In this study, we present an application of ~~new non-destructive~~ method based on gas-permeable tubing and isotope-specific infrared laser absorption spectroscopy *for in situ determination of $\delta^2\text{H}$ and $\delta^{18}\text{O}$* . We conducted a laboratory experiment with an acrylic glass column filled with medium sand equipped with gas-permeable tubing at eight different soil depths. The soil column was initially saturated from the bottom, exposed to evaporation for a period of 290 days, and finally rewatered. Soil water vapor $\delta^2\text{H}$ and $\delta^{18}\text{O}$ were measured daily, sequentially for each depth. Soil liquid water $\delta^2\text{H}$ and $\delta^{18}\text{O}$ were inferred from the isotopic values of the vapor assuming thermodynamic equilibrium between liquid and vapor phases in the soil. The experimental setup allowed following the evolution of typical exponential-shaped soil water $\delta^2\text{H}$ and $\delta^{18}\text{O}$ profiles with unprecedentedly high temporal resolution. As the soil dried ~~out~~, we could also show for the first time the increasing influence of the isotopically depleted ambient water vapor on the isotopically enriched liquid water close to the soil surface (i.e.,

1 atmospheric invasion). Rewatering at the end of the experiment led to instantaneous resetting
2 of the stable isotope profiles, which could be closely followed with the new method.

3 From simple soil $\delta^2\text{H}$ and $\delta^{18}\text{O}$ gradients calculations, we showed that the gathered data
4 allowed to determinate the depth of the Evaporation Front (EF) and how it receded into the
5 soil overtime. It was inferred that after 290 days under the prevailing laboratory air
6 temperature, moisture, and aerodynamic conditions, and given the specific hydraulic
7 properties of the sand, the EF had moved down to an approximate depth of -0.06 m. Finally,
8 data was used to test the expression for the slope of evaporation lines proposed by Gat (1971)
9 and based on the model of Craig and Gordon (1965). A very good agreement was found
10 between measured and simulated values (Nash and Sutcliffe Efficiency - NSE = 0.92) during
11 the first half of the experiment, i.e., until the EF reached a depth of -0.04 m. From this point,
12 calculated kinetic effects associated with the transport of isotopologues in the soil surface air
13 layer above the EF provided slopes lower than observed. Finally, values of isotope kinetic
14 effects that provided the best model-to-data fit (NSE > 0.9) were obtained from inverse
15 modelling, highlighting uncertainties associated with the determinations of isotope kinetic
16 fractionation and soil relative humidity at the EF.~~Finally, from simple soil isotope gradients~~
17 ~~calculations, we showed that the gathered data allowed to determinate the depth at which~~
18 ~~evaporation proceeded in the soil and how this evaporation front receded into the soil with~~
19 ~~time.~~

22 1 Introduction

23 Stable isotopologues of water, namely $^1\text{H}^2\text{H}^{16}\text{O}$ and $^1\text{H}_2^{18}\text{O}$ are powerful tools used in a wide
24 range of research disciplines at different and complementary temporal and spatial scales ~~for,~~
25 They provide ways of e.g., assessing the origin of water vapor (e.g., Craig, 1961; Liu et al.,
26 2010), solving water balances of lakes (Jasechko et al., 2013) and studying groundwater
27 recharge (Blasch and Bryson, 2007; Peng et al., 2014). Analysis of the isotope compositions
28 ($\delta^2\text{H}$ and $\delta^{18}\text{O}$) of soil surface and leaf waters allows for partitioning evapotranspiration into
29 evaporation and transpiration (e.g., Dubbert et al., 2013; Hu et al., 2014; Rothfuss et al., 2012;
30 Yopez et al., 2005).

1 Moreover, from soil water $\delta^2\text{H}$ and $\delta^{18}\text{O}$ profiles, it is also possible to derive quantitative
2 information, such as soil evaporation flux, locate evaporation fronts, and root water uptake
3 depths (Rothfuss et al., 2010; Wang et al., 2010). Zimmermann et al. (1967) and later Barnes
4 and Allison (1983, 1984) and Barnes and Walker (1989) first analytically described soil
5 $^1\text{H}^2\text{H}^{16}\text{O}$ and $^1\text{H}_2^{18}\text{O}$ movement at steady / non-steady state and in isothermal/ non-isothermal
6 soil profiles. Between precipitation events, the soil water $\delta^2\text{H}$ and $\delta^{18}\text{O}$ profiles depend on
7 flux boundary conditions, i.e., fractionating evaporation and non-fractionating capillary rise as
8 well as on soil properties (e.g., soil tortuosity). In a saturated soil, the isotope excess at the
9 surface due to evaporation diffuses back downwards, leading to typical and well documented
10 exponential-shaped $\delta^2\text{H}$ and $\delta^{18}\text{O}$ profiles. For an unsaturated soil, assuming in a first
11 approximation that isotope movement occurs in the vapor phase above the soil “evaporation
12 front” (EF) and strictly in the liquid phase below it, the maximal $\delta^2\text{H}$ and $\delta^{18}\text{O}$ values are no
13 longer observed at the surface but at the depth of EF. Above the EF, in the so-called “vapor
14 region”, ~~by applying according to~~ Fick’s law, soil water $\delta^2\text{H}$ and $\delta^{18}\text{O}$ decrease towards the
15 depleted ambient atmosphere water vapor $\delta^2\text{H}$ and $\delta^{18}\text{O}$. Braud et al. (2005), Haverd and
16 Cuntz (2010), Rothfuss et al. (2012), Singleton et al. (2004), and Sutanto et al. (2012)
17 implemented the description of the transport of $^1\text{H}^2\text{H}^{16}\text{O}$ and $^1\text{H}_2^{18}\text{O}$ in physically based soil-
18 vegetation-atmosphere transfer (SVAT) models (~~Hydrus~~ HYDRUS 1D, SiSPAT-Isotope,
19 Soil-Litter iso, TOUGHREACT). In these models, movement of soil $^1\text{H}^2\text{H}^{16}\text{O}$ and $^1\text{H}_2^{18}\text{O}$
20 occur in both phases below and above the EF, and heat and water transports are properly
21 coupled.

22 However, these tools suffer from the comparison with other “traditional” methods developed
23 to observe and derive soil water state and transport. In contrast with soil water content and
24 tension ~~obtained-measured~~ by, e.g., time-domain reflectometry and tensiometry, isotope
25 compositions of soil water are determined either typically-obtained following destructive
26 sampling or non-destructively but with poor spatial and temporal resolution (i.e., with section
27 cups in combination with lysimeters for soil water tension higher than -600 hPa, e.g.,
28 Goldsmith et al., 2011, Litaor, 1988). This which greatly limits their informative value. Only
29 since recently, non-destructive methodologies based on gas-permeable membrane and laser
30 spectroscopy can be found in the literature (Rothfuss et al., 2013; Herbstritt et al., 2012;
31 Volkman and Weiler, 2014, Gaj et al., 2015).

1 The central objective of this study was to demonstrate that a direct application of the method
2 of Rothfuss et al. (2013) to a soil column would allow monitoring soil water $\delta^2\text{H}$ and $\delta^{18}\text{O}$
3 profiles in the laboratory with high temporal resolution and over a long time period.
4 ~~Furthermore~~ ~~W,~~ ~~we aimed at will~~ demonstrating that the obtained isotope data can be used to
5 locate the evaporation front as it recedes into the soil during the experiment. Finally, data will
6 be also used to test the expression proposed by Gat (1971) and based on the Craig and Gordon
7 (1965) of evaporation lines' slopes.

9 2 Material and methods

10 2.1 Isotopic analyses

11 Isotopic analysis of liquid water and water vapor was performed using a cavity ring-down
12 spectrometer (L1102-i, Picarro, Inc., Santa Clara, CA, USA), calibrated against the
13 international primary water isotope standards V-SMOW2, GISP, and SLAP by liquid water
14 injection into the vaporizer of the analyzer. Primary and working standards' isotope
15 compositions were measured at 17,000 ppmv water vapor mixing ratio (number of replicates
16 = 4, number of injections per replicate = 8). Average-Mean values and standard deviations
17 were calculated omitting the first three values of the first replicate to account for a potential
18 memory effect of the laser spectrometer. The laser spectrometer's dependence on water vapor
19 mixing ratio was also investigated according to the method of Schmidt et al. (2010).
20 Hydrogen and oxygen ~~isotopic-isotope values-ratios~~ of water are expressed in per mil (‰) on
21 the international "delta" scale as defined by Gonfiantini (1978) and referred to as $\delta^2\text{H}$ and
22 $\delta^{18}\text{O}$, respectively.

23 2.2 Soil column and measurements

24 The experiment was conducted in a 0.0057 m³ acrylic glass column (0.11 m i.d., 0.60 m
25 height, Fig. 1a). The bottom of the column consisted of a porous glass plate (10 μm < pore
26 size diameter < 16 μm (4th class), Robu® GmbH, Hattert, Germany) connected to a two-way
27 manual valve (VHK2-01S-06F, SMC Pneumatik GmbH, Germany).

28 Three ports were available at each of eight different depths (-0.01, -0.03, -0.05, -0.07, -0.10,
29 -0.20, -0.40, and -0.60 m): one inlet for the carrier gas, i.e., synthetic dry air (20.5 % O₂ in
30 N₂, with approx. 20-30 ppmv water vapor; Air Liquide, Germany), one sample air outlet, and

1 one duct for a soil temperature (T_s) sensor (type K thermocouple, Greisinger electronic
2 GmbH, Regenstauf, Germany; precision: 0.1°C). An additional fourth port at depths -0.01, -
3 0.03, -0.05, -0.10, -0.20, and -0.60 m was used for the measurement of soil volumetric water
4 content (θ) (EC-5, Decagon Devices, USA; precision: 0.02 m³ m⁻³).

5 At each depth inside the column a 0.15 m long piece of microporous polypropylene tubing
6 (Accurel® PP V8/2HF, Membrana GmbH, Germany; 0.155 cm wall thickness, 0.55 cm i.d.,
7 0.86 cm o.d.) was connected to the gas inlet and outlet port. The tubing offers the two
8 advantages of being gas-permeable (pore size of 0.2 µm) and exhibiting strong hydrophobic
9 properties to prevent liquid water from intruding into the tubing. It allows sampling of soil
10 water vapor and, hence, the determination of the isotope composition of soil liquid water
11 ($\delta_{S_{liq}}$) in a non-destructive manner considering thermodynamic equilibrium between liquid
12 and vapor phases as detailed by Rothfuss et al. (2013).

13 **2.3 Internal isotope standards**

14 Two internal standards (“st1” and “st2”) were prepared using the same procedure as described
15 by Rothfuss et al. (2013). Two closed acrylic glass vessels (0.122 m i.d., 0.22 m height), in
16 each of which a 0.15 meter long piece of tubing as well as a type K thermocouple were
17 installed, were filled with FH31 sand (porosity = 0.34 m³ m⁻³, dry bulk density = 1.69 g cm³,
18 particle size distribution: 10% (>0.5 mm), 72% (0.25-0.5 mm), and 18% (<0.25 mm)) (Merz
19 et al., 2014; Stingaciu et al., 2009). Each vessel was saturated with water of two different
20 isotope compositions: $\delta^2H_{st1} = -53.51 (\pm 0.10) \text{‰}$, $\delta^{18}O_{st1} = -8.18 (\pm 0.06) \text{‰}$ and $\delta^2H_{st2} =$
21 $+15.56 (\pm 0.12) \text{‰}$, $\delta^{18}O_{st2} = +8.37 (\pm 0.04) \text{‰}$. Soil water vapor from each vessel was
22 sampled eight times per day for 30 min during the whole experiment.

23 **2.4 Atmospheric measurements**

24 Laboratory air was sampled passively with a 1/8” three meter-long stainless steel tubing at 2
25 m above the sand surface for isotope analysis of water vapor (δ_a). Air relative humidity (rh)
26 and temperature (T_a) were monitored at the same height with a combined rh and T_a sensor
27 (RFT-2, UMS GmbH, Germany; precision for rh and T_a were 2 % and 0.1°C, respectively).
28 Vapor pressure deficit (vpd) was calculated from rh and T_a data using the Magnus-Tetens
29 formula (Murray, 1967) for saturated vapor pressure. The laboratory was air-conditioned and

1 ventilated with seven axial fans (ETRI 148VK0281, 117 l s⁻¹ airflow, ETRI/Rosenberg, USA)
2 positioned at 1.80 m height above the sand surface.

3 **2.5 Sampling protocol and applied isotopic calibrations**

4 The column was filled in a single step with FH31 sand and carefully shaken in order to reach
5 a dry bulk density close to *in situ* field conditions. The sand was then slowly saturated from
6 the bottom from an external water tank filled with st1 water on December 2, 2013. After
7 saturation, the column was disconnected and sealed at the bottom using the two-way manual
8 valve. It was finally installed on a balance (Miras 2 – 60EDL, Sartorius, USA), and let to
9 evaporate for a period of 290 days in a ventilated laboratory.

10 δ_{Sliq} was determined in a sequential manner at each available depth once a day following the
11 method developed by Rothfuss et al. (2013) (Fig. 1b). Dry synthetic air at a rate of 50 ml min⁻¹
12 from a mass flow controller (EL-FLOW Analog, Bronkhorst High Tech, Ruurlo, The
13 Netherlands) was directed to the permeable tubing for 30 minutes at each depth. The sampled
14 soil water vapor was diluted with dry synthetic air provided by a second mass flow controller
15 of the same type. ~~This allowed in order to~~ (i) reaching a water vapor mixing ratio value
16 ranging between 17,000 and 23,000 ppmv (where L1102-i isotope measurements are most
17 precise) and (ii) ~~generate-generating~~ an excess flow downstream of the laser ~~analyzer~~ ~~analyser~~.
18 ~~By doing this, a to avoid a~~ any contamination of sample air with ambient air ~~would be avoided~~.
19 The excess flow was measured with a digital flow meter (ADM3000, Agilent Technologies,
20 Santa Clara, CA, USA). The last 100 observations (corresponding to approx. 10 minutes) at
21 steady state (standard deviations <0.70 ‰ and <0.20 ‰ for $\delta^2\text{H}$ and $\delta^{18}\text{O}$, respectively) were
22 used to calculate the raw isotope compositions of soil water vapor (δ_{Svap}). ~~The latter was~~
23 ~~correcting~~ for the water vapor mixing ratio dependence of the laser analyzer readings with
24 17,000 ppmv as reference level. ~~Measurements that did not fulfil the above mentioned~~
25 ~~conditions for $\delta^2\text{H}$ and $\delta^{18}\text{O}$ standard deviations were not taken into account~~. Finally, these
26 corrected values were used to infer the corresponding δ_{Sliq} at the measured T_{S} (Eq. (1) and (2);
27 taken from Rothfuss et al., 2013):

$$28 \quad \delta^2\text{H}_{\text{Sliq}} = 104.96 - 1.0342 \cdot T_{\text{S}} + 1.0724 \cdot \delta^2\text{H}_{\text{Svap}} \quad (1)$$

$$29 \quad \delta^{18}\text{O}_{\text{Sliq}} = 11.45 - 0.0795 \cdot T_{\text{S}} + 1.0012 \cdot \delta^{18}\text{O}_{\text{Svap}} \quad (2)$$

1 The isotope composition of laboratory water vapor (δ_a) was measured eight times a day. δ_a ,
2 δ_{svap} and δ_{slq} values were finally corrected for laser instrument drift with time, using the
3 isotope compositions of the two water standards, δ_{st1} and δ_{st2} .

4 Water vapor of the ambient air, of both standards, and from the different tubing sections in the
5 soil column were sampled sequentially in the following order: soil (0.60 m) – soil (0.40 m) –
6 atmosphere – st1 – st2 – soil (0.20 m) – soil (0.10 m) – atmosphere – st1 – st2 – soil (0.07 m)
7 – soil (0.05 m) – atmosphere – st1 – st2 – soil (0.03 m) – soil (0.01 m). Atmosphere water
8 vapor was sampled twice as long (i.e., one hour) as soil water vapor from the
9 column/standards so that each sequence lasted exactly 10 hours and started each day at the
10 same time. The remaining 14 hours were used for additional standard and atmosphere water
11 vapor measurements (i.e., on five occasions each).

12 **2.6 Irrigation event**

13 On Day of Experiment (DoE) 290 at 09:30 the sand surface was irrigated with 70 mm of st1
14 water. This was achieved over one hour in order to avoid oversaturation of the sand and avoid
15 preferential pathways that would have affected the evaporation rate. For this, a 2 L
16 polyethylene bottle was used. Its bottom was perforated with a set of 17 holes of 5 mm
17 diameter and its cap with a single hole through which a PTFE bulkhead union tube fitting
18 (Swagelok, USA) was installed. The bulkhead fitting was connected to a two-way needle
19 valve (Swagelok, USA). Opening/closing the valve controlled the flow rate at which air
20 entered the bottle headspace, which in turn controlled the ~~for adjusting~~ the irrigation flow
21 rate.

22 To better observe the dynamics directly following the irrigation event, water vapor was
23 sampled at a higher rate, i.e., 1, 3, 4, 5, 6, 9, 11, and 11 times per day at –0.60, –0.40, –0.20, –
24 0.10, –0.07, –0.05, –0.03, and –0.01 m. Water vapor from both standards was sampled twice a
25 day. The experiment was terminated after 299 days on September 26th, 2014.

26 **2.7 Evaporation lines (Craig and Gordon model, 1965)**

27 Gat et al. (1971) proposed an expression based on the model of Craig and Gordon (1965) for
28 the slope of the so-called “evaporation line” (S_{Ev}) which quantifies the relative change in $\delta^2\text{H}$
29 and $\delta^{18}\text{O}$ in a water body undergoing evaporation:

$$S_{Ev} = \frac{\Delta(\delta^2\text{H}_{\text{Sliq}})}{\Delta(\delta^{18}\text{O}_{\text{Sliq}})} = \frac{rh \cdot (\delta^2\text{H}_a - \delta^2\text{H}_{\text{Sliq_ini}}) + \varepsilon_{\text{eq}}^{2\text{H}} + \Delta\varepsilon^{2\text{H}}}{rh \cdot (\delta^{18}\text{O}_a - \delta^{18}\text{O}_{\text{Sliq_ini}}) + \varepsilon_{\text{eq}}^{18\text{O}} + \Delta\varepsilon^{18\text{O}}} \quad (3)$$

where $\Delta\varepsilon^{2\text{H}}$ (resp. $\Delta\varepsilon^{18\text{O}}$) is the so-called “isotope kinetic effect” associated with $^1\text{H}^2\text{H}^{16}\text{O}$ (resp. $^1\text{H}_2^{18}\text{O}$) vapor transport:

$$\Delta\varepsilon^{2\text{H}} = (1 - rh) \cdot \varepsilon_{\text{K}}^{2\text{H}} \quad (4a)$$

$$\Delta\varepsilon^{18\text{O}} = (1 - rh) \cdot \varepsilon_{\text{K}}^{18\text{O}} \quad (4b)$$

$\delta^2\text{H}_{\text{Sliq_ini}}$ (resp. $\delta^{18}\text{O}_{\text{Sliq_ini}}$) is the initial soil liquid $\delta^2\text{H}$ (resp. $\delta^{18}\text{O}$), i.e., prior removal of water vapor by fractionating evaporation. $\varepsilon_{\text{eq}}^{2\text{H}}$ (resp. $\varepsilon_{\text{eq}}^{18\text{O}}$) and $\varepsilon_{\text{K}}^{2\text{H}}$ (resp. $\varepsilon_{\text{K}}^{18\text{O}}$) are the equilibrium and kinetic $^1\text{H}^2\text{H}^{16}\text{O}$ (resp. $^1\text{H}_2^{18}\text{O}$) enrichments. $\varepsilon_{\text{eq}}^{2\text{H}}$ (resp. $\varepsilon_{\text{eq}}^{18\text{O}}$) is defined by the deviation from unity of the ratio between water and $^1\text{H}^2\text{H}^{16}\text{O}$ (resp. $^1\text{H}_2^{18}\text{O}$) saturated vapor pressures and can be calculated using the empirical closed-form equations proposed by, e.g., Majoube (1971). $\varepsilon_{\text{K}}^{2\text{H}}$ (resp. $\varepsilon_{\text{K}}^{18\text{O}}$) is defined as the deviation from unity of the ratio between the resistance associated with the transport of $^1\text{H}^2\text{H}^{16}\text{O}$ (resp. $^1\text{H}_2^{18}\text{O}$) vapor in the boundary air layer above the evaporating surface and that of water vapor. By assuming that (i) turbulent transport is a non-fractionating process and (ii) resistance associated with molecular diffusion of $^1\text{H}^2\text{H}^{16}\text{O}$ (resp. $^1\text{H}_2^{18}\text{O}$) vapor is inversely proportional to the n^{th} power of the corresponding diffusivity ($D^{2\text{H}}$, resp. $D^{18\text{O}}$), Merlivat and Coantic (1975) proposed the following expressions:

$$\varepsilon_{\text{K}}^{2\text{H}} = \left(\frac{D}{D^{2\text{H}}} \right)^n - 1 = (1.0251)^n - 1 \quad (5a)$$

$$\varepsilon_{\text{K}}^{18\text{O}} = \left(\frac{D}{D^{18\text{O}}} \right)^n - 1 = (1.0285)^n - 1 \quad (5b)$$

The exponent n accounts for the aerodynamic regime above the liquid–vapor interface (i.e., where the relative humidity is 100%) and ranges from $n_a = 0.5$ (fully turbulent, i.e., atmosphere-controlled conditions) to $n_s = 1$ (fully diffusive, i.e., soil-controlled conditions) with a value of $\frac{2}{3}$ corresponding to laminar flow conditions (Dongmann et al., 1974,

1 Brutsaert, 1975). In the present study, values for ratios of diffusivities ($D/D^{2\text{H}}$ and $D/D^{18\text{O}}$)
2 were taken from Merlivat (1978) and n was considered as a function of soil water content as
3 proposed by Mathieu and Bariac (1996):

$$4 \quad n = \frac{(\theta_{\text{surf}} - \theta_{\text{res}}) \cdot n_a + (\theta_{\text{sat}} - \theta_{\text{res}}) \cdot n_s}{\theta_{\text{sat}} - \theta_{\text{res}}} \quad (6)$$

5 with θ_{res} , θ_{sat} , and θ_{surf} the residual, saturated and surface soil water contents ($\text{m}^3 \text{m}^{-3}$).

6 Note that Equation (3) contrasts with the expression for the slope characterizing equilibrium
7 processes (e.g., precipitation formation) and therefore strictly temperature-dependant (i.e.,

8 $S_{\text{eq}} = \varepsilon_{\text{eq}}^{2\text{H}} / \varepsilon_{\text{eq}}^{18\text{O}}$). While S_{eq} might range for instance from 7.99 to 8.94 (for temperatures

9 spanning between 5 and 30°C), a much wider spread in S_{Ev} values is possible and has been

10 measured between 2 and 6 (Barnes and Allison, 1988, Brunel et al., 1995, DePaolo et al.,

11 2004).

12 **3 Results**

13 **3.1 Example of a measuring sequence**

14 Figure 2 shows exemplarily the measuring sequence for DoE 150. Soil and standards water
15 vapor mixing ratios were stable and ranged ~~between~~ from 17,200 ~~and to~~ 18,200 ppmv during
16 the last 10 minutes of each sampling period (Fig. 2a). δ_{Svap} was within the range spanned by
17 δ_{st1vap} and δ_{st2vap} for both ^2H and ^{18}O (Fig. 2b). On DoE 150, the soil surface was sufficiently
18 dry so that atmospheric invasion of water vapor had started to significantly influence the δ_{Svap}
19 of the upper soil layers. Therefore, δ_{Svap} measured at -0.01 m was lower than at -0.03 m for
20 both ^2H and ^{18}O , but less pronounced for ^2H .

21 **3.2 Time courses of air temperature, relative humidity and atmospheric $\delta^2\text{H}$** 22 **and $\delta^{18}\text{O}$**

23 During the experiment, the laboratory air temperature ranged from 15.6 to 22.5 °C (average:
24 18.7 ± 1.5 °C, Fig. 3a) and the relative humidity from 19 to 69 % (average: $40 \% \pm 0.08 \%$,
25 Fig. 3a). Lower values of δ_a were observed from DoE 0 to 125 at lower air temperatures,
26 whereas higher values occurred after DoE 125 at higher air temperatures (Fig. 3b).

1 3.3 Evolution of soil water content, temperature, evaporation flux, and δ_{Svap} 2 from DoE 0-290

3 The soil temperature ranged from 16.2 to 22.3 °C (average: 18.6 ± 1.3 °C, data not shown)
4 and closely followed that in the air, i.e., differences between daily mean soil and air
5 temperatures ranged from -0.2 to 0.2 °C during the experiment. Following the saturation of
6 the column, a strong decrease in water content was observed in the upper 10 cm, whereas
7 after 287 days the sand was still saturated at -0.60 m (Fig. 4a). Figure 4b shows the time
8 series of evaporation flux normalized by the vapor pressure deficit in the laboratory air
9 (Ev/vpd , expressed in $\text{mm day}^{-1} \text{ kPa}^{-1}$). Ev/vpd ratio was high at the beginning of the
10 experiment, i.e., ranged from 2.44 to $3.22 \text{ mm d}^{-1} \text{ kPa}^{-1}$ during the first two experimental
11 days. After DoE 180 and until the soil was irrigated, Ev/vpd stabilized to a mean value of 0.03
12 (± 0.02) $\text{mm d}^{-1} \text{ kPa}^{-1}$.

13 Due to fractionating evaporation flux, the δ_{Svap} of the topmost layer (-0.01 m) increased
14 instantaneously (i.e., from DoE 0 onward) from the equilibrium δ_{Svap} value with the input
15 water (-17.3 ‰ and -132.3 ‰ for ^{18}O and ^2H , respectively, at 16.5°C, Fig. 4c and d).
16 Through back-diffusion of the excess heavy stable isotopologues from the evaporation front,
17 δ_{Svap} measured at depths -0.03, -0.05, -0.07, -0.10, and -0.20 m departed from that same
18 equilibrium value after 2, 3, 10, 25, and 92 days of the experiment, respectively. On the other
19 hand, δ_{Svap} of the layers -0.40 and -0.60 m were constant over the entire duration of the
20 experiment. Until DoE 65, the δ_{Svap} of the first 10 cm increased. From DoE 65 to 113 δ_{Svap}
21 reached an overall stable value in the top layers -0.01 m ($\delta^2\text{H}_{\text{Svap}} = 4.82 \pm 2.06$ ‰; $\delta^{18}\text{O}_{\text{Svap}} =$
22 11.72 ± 0.67 ‰) and -0.03 m ($\delta^2\text{H}_{\text{Svap}} = 5.61 \pm 3.14$ ‰; $\delta^{18}\text{O}_{\text{Svap}} = 10.41 \pm 0.81$ ‰), whereas
23 δ_{Svap} measured at depths -0.05, -0.07, and -0.10 m still progressively increased; from DoE 72
24 onward, δ_{Svap} at -0.20 m started to increase. $\delta^2\text{H}_{\text{Svap}}$ and $\delta^{18}\text{O}_{\text{Svap}}$ values started to decrease
25 after about DoE 113 and DoE 155, respectively. $\delta^2\text{H}_{\text{Svap}}$ at -0.01, -0.03, and -0.07 m on the
26 one hand and $\delta^{18}\text{O}_{\text{Svap}}$ at -0.01, -0.03, and -0.07 m on the other followed similar evolutions
27 with maximum values measured below the surface down to -0.05 m.

28 3.4 Evolution of soil water content, temperature, evaporation flux, and δ_{Svap} 29 from DoE 290 to 299

30 The layers -0.01, -0.03, -0.05, -0.10, and -0.20 m showed increases in θ of 0.31, 0.22, 0.30,
31 0.23, and $0.16 \text{ m}^3 \text{ m}^{-3}$ following irrigation, whereas θ at -0.60 m remained constant (Fig. 4e).

1 $\theta_{-0.01\text{m}}$ and $\theta_{-0.03\text{m}}$ rapidly decreased down to values of 0.12 and 0.13 $\text{m}^3 \text{m}^{-3}$. Note that when
2 $\theta_{-0.01\text{m}}$ and $\theta_{-0.03\text{m}}$ reached these values prior to irrigation, the evaporation rate was similar
3 (i.e., $Ev/vpd = 0.65 (\pm 0.12) \text{ mm d}^{-1}$, Fig. 4f).

4 Immediately after irrigation and for both isotopologues, δ_{Svap} at -0.01 , -0.03 , and -0.05 m
5 was reset to a value close to that in equilibrium with st1 water (i.e., -17.8 ‰ and -132.0 ‰
6 for ^{18}O and ^2H , respectively, at 21.8 °C soil temperature, Fig. 4g and h). At -0.07 m, δ_{Svap}
7 reached the above mentioned equilibrium values after about 3.5 days. δ_{Svap} at -0.20 m evolved
8 in a similar way, whereas at -0.10 m the equilibrium values were reached after six hours.
9 Finally, δ_{Svap} at -0.40 and -0.60 m and for both isotopologues were not affected by the water
10 addition, which was consistent with the observed θ changes.

11 **3.5 Evolution of soil temperature, water content, and δ_{Sliq} profiles**

12 In Figure 5, T_s , θ , and δ_{Sliq} profiles for both isotopologues are plotted in three different panels,
13 from DoE 0 to 100 (Fig. 5a-d, top panels), from DoE 101 to 287 (Fig. 5e-h, center panels),
14 and from DoE 288 to 299 (Fig. 5i-l, bottom panels). The represented profiles were obtained
15 from a linear interpolation of the times series of each variable. Thus, since the measuring
16 sequence started each day at 08:00 and ended at 18:00, the depicted profiles are centered on
17 13:00.

18 Even if the soil temperature fluctuated during the course of the experiment, quasi-isothermal
19 conditions were fulfilled at a given date, as the column was not isolated from its surroundings.
20 On average, T_s only varied by 0.2 °C around the profile mean temperature at a given date.
21 The δ_{Sliq} profiles showed a typical exponential shape from DoE 0 to approx. 100. Around DoE
22 100, when θ at -0.01 m reached a value of $0.090 \text{ m}^3 \text{m}^{-3}$ (i.e., significantly greater than the
23 sand residual water content $\theta = 0.035 \text{ m}^3 \text{m}^{-3}$, determined by Merz et al. (2014)), the maximal
24 δ_{Sliq} values were no longer observed at the surface and atmosphere water vapor started
25 invading the first centimeter of soil. Note that this happened slightly faster for $^1\text{H}^2\text{H}^{16}\text{O}$ than
26 for $^1\text{H}_2^{18}\text{O}$. On DoE 290, when the column was irrigated, the isotope profiles were partly reset
27 to their initial state, i.e., constant over depth and close to -53.5 and -8.2 ‰ for $^1\text{H}^2\text{H}^{16}\text{O}$ and
28 $^1\text{H}_2^{18}\text{O}$, respectively, with the exception of still enriched values at -0.07 m.

3.6 $\delta^2\text{H}$ - $\delta^{18}\text{O}$ relationships in soil water and atmosphere water vapor

Each plot of Figure 6 represents data of 50 consecutive days of the experiment. Laboratory atmosphere water vapor $\delta^2\text{H}$ and $\delta^{18}\text{O}$ (gray symbols) were linearly correlated (linear regression relationships in gray dotted lines) during the entire experiment (R^2 ranging between 0.74 and 0.90, F-statistic p-value < 0.01), with the exception of the period DoE 125-155 ($R^2 = 0.31$, $p < 0.001$), when atmospheric water vapour $\delta^2\text{H}$ was remarkably high in the laboratory (Fig. 6c and d).

The linear regression slopes (LRS) between $\delta^2\text{H}_a$ and $\delta^{18}\text{O}_a$ ranged from 6.20 (DoE 50-100, $p < 0.01$) to 8.29 (DoE 0-50, gray dotted line, $p < 0.001$). These values were significantly lower than S_{eq} , the calculated ratio between the liquid-vapor equilibrium fractionations of $^1\text{H}^2\text{H}^{16}\text{O}$ and $^1\text{H}_2^{18}\text{O}$ (Majoube, 1971) that characterizes meteoric water bodies, which should have ranged from 8.41 to 8.92 at the measured monthly mean atmosphere temperatures (Forschungszentrum Jülich wheat station, $6^\circ24'34''$ E, $50^\circ54'36''$ N, 91 m.a.s.l.). Therefore, it can be deduced that the laboratory air moisture was partly resulting from column evaporation, typically leading to a $\delta^2\text{H}$ - $\delta^{18}\text{O}$ regression slope of lower than eight. This also highlights the particular experimental conditions in the laboratory, where other sources of water vapour (e.g., by opening the laboratory door) might have influenced the isotope compositions of the air.

Considering all soil depths, the $\delta^2\text{H}_{\text{Sliq}}-\delta^{18}\text{O}_{\text{Sliq}}$ LRS increased from 2.96 to 4.86 over the course of the experiment (with $R^2 > 0.89$, $p < 0.001$). These values were much lower than that of the slope of the Global Meteoric Water Line (GMWL, i.e., slope=8) also represented in Figure 6. However, Figure 6 highlights the fact that in the upper three layers (-0.01, -0.03, and -0.05 m) $\delta^2\text{H}_{\text{Sliq}}-\delta^{18}\text{O}_{\text{Sliq}}$ LRS followed a significantly different evolution as the soil dried out. Figure 7 shows average $\delta^2\text{H}$ - $\delta^{18}\text{O}$ LRS calculated for time intervals of ten consecutive days for the atmosphere (gray line), the three upper layers (colored solid lines), and the remaining deeper layers (-0.07, -0.10, -0.20, -0.40, and -0.60 m, black dotted line). While both $\delta^2\text{H}$ - $\delta^{18}\text{O}$ LRS in the atmosphere and in the first three depths fluctuated during the experiment, the LRS of the combined remaining deeper layers varied only little between 3.07 and 4.49 (average = 3.78 ± 0.54). From DoE 150, $\delta^2\text{H}$ - $\delta^{18}\text{O}$ LRS of the atmosphere and at -0.01, -0.03, and -0.05 m were linearly correlated ($R^2 = 0.73$, 0.48, and 0.42, with $p < 0.001$, < 0.01, and < 0.05, respectively), whereas they were not correlated before DoE 125, demonstrating again the increasing influence of the atmosphere (atmosphere invasion) on the

1 soil surface layer as the EF receded in the soil. Note the negative $\delta^2\text{H}_a$ - $\delta^{18}\text{O}_a$ LRS ($R^2 = 0.26$,
2 $p < 0.001$) observed between DoE 125 and 150, due to remarkably high atmosphere vapor
3 $\delta^2\text{H}$ measured in the laboratory.

4 **4 Discussion**

6 **4.1 Long term reliability of the method**

7 The method proved to be reliable in the long term as the tubing sections positioned at -0.60
8 and -0.40 m (i.e., where the sand was saturated or close to saturation during the entire
9 experiment) remained watertight even after 299 days. As demonstrated by Rothfuss et al.
10 (2013), (i) the length of the gas-permeable tubing, (ii) the low synthetic dry air flow rate, and
11 (iii) the daily measurement frequency allowed removing soil water vapor which remained
12 under thermodynamic equilibrium with the soil moisture. Moreover, this was also true for the
13 upper soil layers even at ~~very~~ low soil water content: steady values for water vapor mixing
14 ratio and isotope compositions were always reached during sampling throughout the
15 experiment. Finally, our method enabled inferring the isotope composition of ~~very~~ tightly
16 bound water at the surface, ~~which~~ This would be observable by the traditional vacuum
17 distillation method with certainly a lower vertical resolution due to ~~very~~ low moisture content.
18 As also pointed out by Rothfuss et al. (2013), it can be assumed that the sand properties did
19 not cause any fractionation of pore water ^2H and ^{18}O . In contrast, this could not be the case in
20 certain soils with high cation exchange capacity (CEC) as originally described by Sofer and
21 Gat (1972) and recently investigated by Oerter et al. (2014).

22 ~~4.2 $\delta^2\text{H}$ - $\delta^{18}\text{O}$ relationships in soil water and atmosphere water vapor~~

23 ~~Each plot of Figure 6 represents data of 50 consecutive days of the experiment. Atmosphere~~
24 ~~water vapor $\delta^2\text{H}$ and $\delta^{18}\text{O}$ (gray symbols) were linearly correlated (linear regression~~
25 ~~relationships in gray dotted lines) during the entire experiment (R^2 ranging between 0.7 and~~
26 ~~0.9), with the exception of the period DoE 125-155, when atmospheric $\delta^2\text{H}$ was remarkably~~
27 ~~high in the laboratory (Fig. 6c and d).~~

28 ~~The linear regression slopes (LRS) between $\delta^2\text{H}_a$ and $\delta^{18}\text{O}_a$ ranged from 6.20 (DoE 50-100) to~~
29 ~~8.29 (DoE 0-50, gray dotted line). These values were significantly lower than the calculated~~
30 ~~ratio of the equilibrium fractionation for $^1\text{H}^2\text{H}^{16}\text{O}$ and $^1\text{H}_2^{18}\text{O}$ that characterizes meteoric~~

1 water bodies, which should have ranged between 8.32 (DoE 200-250) and 8.47 (DoE 0-50) at
2 the measured laboratory air temperatures. Therefore, it can be deduced that the laboratory air
3 moisture was partly resulting from column evaporation, typically leading to a $\delta^2\text{H}$ - $\delta^{18}\text{O}$
4 regression slope of lower than eight.

5 Considering all soil depths, the $\delta^2\text{H}_{\text{Sliq}}$ - $\delta^{18}\text{O}_{\text{Sliq}}$ -LRS increased from 2.96 to 4.86 over the
6 course of the experiment (with $R^2 > 0.89$). However, Figure 6 highlights the fact that in the
7 upper three layers (0.01, 0.03, and 0.05 m) $\delta^2\text{H}_{\text{Sliq}}$ - $\delta^{18}\text{O}_{\text{Sliq}}$ -LRS followed a significantly
8 different evolution as the soil dried out. Figure 7 shows average $\delta^2\text{H}$ - $\delta^{18}\text{O}$ -LRS calculated for
9 time intervals of ten consecutive days for the atmosphere (gray line), the three upper layers
10 (colored solid lines), and the remaining deeper layers (0.07, 0.10, 0.20, 0.40, and 0.60
11 m, black dotted line). While both $\delta^2\text{H}$ - $\delta^{18}\text{O}$ -LRS in the atmosphere and in the first three
12 depths fluctuated during the experiment, the LRS of the combined remaining deeper layers
13 varied only little between 3.07 and 4.49 (average = 3.78 ± 0.54). From DoE 150, $\delta^2\text{H}$ - $\delta^{18}\text{O}$
14 LRS of the atmosphere and at 0.01, 0.03, and 0.05 m were linearly correlated ($R^2 = 0.73$,
15 0.48, and 0.42, respectively), whereas they were not correlated before DoE 125,
16 demonstrating again the increasing influence of the atmosphere (atmosphere invasion) on the
17 soil surface layer as the EF receded in the soil. Note the absence of $\delta^2\text{H}_a$ - $\delta^{18}\text{O}_a$ -linear
18 correlation (LRS < 0 , with negative R^2) observed between DoE 125 and 150, due to
19 remarkably high atmosphere vapor $\delta^2\text{H}$ measured in the laboratory.

20 **4.34.2 Locating the evaporation front depth from soil water $\delta^2\text{H}$ and $\delta^{18}\text{O}$** 21 **profiles**

22 From Figure 4b no distinct characteristic evaporation stages, i.e., stages I and II referring to
23 atmosphere-controlled and soil-controlled evaporation phases, respectively, could be
24 identified. The opposite was observed by as opposed to Merz et al. (2014), who conducted an
25 evaporation study using the same sand. This indicates greater wind velocity in the air layer
26 above the soil column due to the laboratory ventilation. For higher wind velocities, the
27 boundary layer above the drying medium is thinner and the transfer resistance for vapor
28 transfer lower than for lower wind velocities. But, for thinner boundary layers, the
29 evaporation rates depends stronger on the spatial configuration of the vapor field above the
30 partially wet evaporating surface. This makes that the evaporation rate decreases and the
31 transfer resistance in the boundary layer increases more in relative terms with decreasing
32 water content of the evaporation surface for higher than for lower wind velocities (Shahraeeni

~~et al., 2012). This indicates greater wind velocity in the air layer above the soil column due to the laboratory ventilation system which would lead to a decrease in evaporation rate during stage I due to an increased transfer resistance in the boundary layer above the drying porous medium as observed and modelled by Shahraneini et al. (2012).~~

Locating the EF in the soil is of importance for evapotranspiration partitioning purposes: from the soil water isotope composition at the EF, it is possible to calculate the evaporation flux isotope composition using the Craig and Gordon formula (Craig and Gordon, 1965). For a uniform isotope diffusion coefficient distribution in the liquid phase, an exponential decrease of the isotope composition gradient with depth is expected. However, when evaporation and thus accumulation of isotopologues occur in a soil layer between two given observation points, then the isotope gradient between these two points is smaller than the gradient deeper in the profile. Therefore we can consider the time when the isotope composition gradient is no longer the largest between these two upper observation depths as the time when the EF moves into the soil layer below.

Figure 8a and b display the evolutions of the isotope compositions gradients $d(\delta^{18}O_s)/dz$ and $d(\delta^2H_s)/dz$ calculated between two consecutive observation points in the soil (i.e., between -0.01 and -0.03 m in brown solid line, between -0.03 and -0.05 m in red solid line, etc.). Figure 8c translates these isotope gradients in terms of EF depths ($z^{18}O_{EF}$ and z^2H_{EF} , respectively). Each day, the maximum $d(\delta^{18}O_s)/dz$ and $d(\delta^2H_s)/dz$ define the layer where evaporation occurs, e.g., when $d(\delta^{18}O_s)/dz$ is maximal between -0.01 and -0.03 m on a given DoE, $z^{18}O_{EF}$ is estimated to be greater than -0.01 m and is assigned the value of 0 m. When $d(\delta^{18}O_s)/dz$ is maximal between -0.03 and -0.05 m on a given DoE, $z^{18}O_{EF}$ is estimated to range between ~~than~~ -0.01 and -0.03 m and is assigned the value -0.02 m. From both $d(\delta^{18}O_s)/dz$ and $d(\delta^2H_s)/dz$, a similar evolution of the depth of the evaporation front was derived despite the fact that $\delta^{2}H_{sliq}$ and $\delta^{18}O_{sliq}$ time courses were different and showed maxima at different times. It was inferred that after 290 days under the prevailing laboratory air temperature, moisture, and aerodynamic conditions, and given the specific hydraulic properties of the sand, the EF had moved down to an approximate depth of -0.06 m.

4.3 Testing the Craig and Gordon (1965) relationship with isotope data

For each period of ten consecutive days the minimum measured $\delta^2\text{H}_{\text{Sliq}}$ and $\delta^{18}\text{O}_{\text{Sliq}}$ provided $\delta^2\text{H}_{\text{Sliq}_{\text{ini}}}$ and $\delta^{18}\text{O}_{\text{Sliq}_{\text{ini}}}$ in Equation (3). $\delta^2\text{H}_a$ and $\delta^{18}\text{O}_a$ were obtained from the mean values of their respective times series. Mean soil surface water content (θ_{surf}) measured in the layer above the EF (as identified in section 4.2) provided the n parameter in Equation (6) and ultimately $\varepsilon_{\text{K}}^{2\text{H}}$ and $\varepsilon_{\text{K}}^{18\text{O}}$ (Eq. (5a) and (5b)). $\varepsilon_{\text{eq}}^{2\text{H}}$ and $\varepsilon_{\text{eq}}^{18\text{O}}$ were calculated from Majoube (1971) at the mean soil temperature measured at z_{EF} . Relative humidity was normalized to the soil temperature measured at the EF. Finally, standard error for S_{Ev} was obtained using an extension of the formula proposed by Phillips and Gregg (2001) and detailed by Rothfuss et al. (2010). For this, standard errors associated with the determination of the variables in Equation (3) were taken equal to their measured standard deviations for each time period. Standard errors for the parameters θ_{res} and θ_{sat} were set arbitrarily to $0.01 \text{ m}^3 \text{ m}^{-3}$ and for the diffusivity ratios $D/D^{2\text{H}}$ and $D/D^{18\text{O}}$ to zero (i.e., no uncertainty about their value was taken into account, although debatable, e.g., Cappa et al., 2003).

Figure 9a shows the comparison between time courses of S_{Ev} and $\delta^2\text{H}_{\text{Sliq}}\text{-}\delta^{18}\text{O}_{\text{Sliq}}$ LRS computed with data below the EF. Both ranged between 2.9 and 4.8, i.e., within the range of reported values (e.g., Barnes and Allison, 1988, Brunel et al., 1995, DePaolo et al., 2004). Note that both observed and simulated slopes' values increased over time, even though the boundary air layer above the EF gradually thickened as the soil dried out. The opposite was observed by e.g., Barnes and Allison (1983), who simulated isotopic profiles at steady state with constant relative humidity. In the present study however the atmosphere relative humidity gradually increased which in turn decreased the kinetic effects associated with $^1\text{H}^2\text{H}^{16}\text{O}$ and $^1\text{H}_2^{18}\text{O}$ vapour transports and thus increased slopes over time. The general observed trend was very well reproduced by the model between DoE 30 and 150 (Nash and Sutcliffe Efficiency - NSE = 0.92; Nash and Sutcliffe, 1970), whereas S_{Ev} departed from data from DoE 150 onwards (NSE < 0). Overall, the Craig and Gordon (1965) model could explain about 62 % of the data variability with a Root Mean Square Error (RMSE) of 0.58 (and 76 % when data from the period DoE 0-10 is left out, p-value < 0.001, RMSE = 0.52). At the beginning of the experiment (DoE 0-20), simulated values were greater than computed $\delta^2\text{H}\text{-}\delta^{18}\text{O}$ LRS, even when taking into account the high S_{Ev} standard errors due to fast changing θ_{surf} (Phillips and Gregg, 2001). Although S_{Ev} was equal to 3.8 for the period DoE 0-10, $\delta^2\text{H}\text{-}\delta^{18}\text{O}$ LRS had already reached down a value of 2.9, meaning that the EF should have

1 been no longer at the surface (i.e., between the surface and 0.01 m depth) leading to greater n,
2 therefore lower slope value.

3 After DoE 150 and until DoE 290 when evaporation flux was lower than 0.40 mm d⁻¹,
4 difference between model and data progressively increased. For a better model-to-data fit, the
5 ¹H²H¹⁶O and ¹H₂¹⁸O kinetic effects should decrease, through either (i) decrease of ϵ_K (i.e.,
6 decrease of n), which is from a theoretical point of view counter-intuitive and e.g., contradicts
7 the formulation of Mathieu and Bariac (1996) or (ii) decrease of term $(1 - rh)$, or else (iii) a
8 combination of (i) and (ii). In another laboratory study where $\delta^{18}\text{O}$ of water in bare soil
9 columns was measured destructively and $\delta^{18}\text{O}$ of evaporation was estimated from cryoscopic
10 trapping of water vapour at the outlet of the columns' headspaces, Braud et al. (2009a and b)
11 could capture $\epsilon_K^{18\text{o}}$ dynamics by inverse modelling. In their case, $\epsilon_K^{18\text{o}}$ generally reached values
12 close to $\epsilon_K^{18\text{o}} = 18.9\text{‰}$ corresponding to laminar conditions above the liquid-vapor interface (n
13 = 2/3). They however determined at the end of their experiments, when the soil surface dry
14 layer thickened and soil surface relative humidity was significantly lower than 100%, values
15 lower than reported in the literature (i.e., $\epsilon_K^{18\text{o}} < 14.1\text{‰}$). These results were partly explained
16 by the particular experimental conditions leading to uncertainties in characterizing
17 evaporation isotope compositions when the dry soil surface layer was the most developed.
18 Nevertheless, the same observation could be made in the present study while having a
19 different soil texture (silt loam *versus* quartz sand) and noticeable different atmospheric
20 conditions ("free" laboratory atmosphere *versus* sealed headspace circulated with dry air).
21 Figure 9c displays the evolution of $\epsilon_K^{2\text{H}}$ (resp. $\epsilon_K^{18\text{o}}$) that provided the best fit with data (NSE =
22 0.99) through fitting of the n parameter (shown Figure 9b) instead of calculating it with
23 Equation (6). In this scenario, n decreased from one to 0.59, with a mean value of 0.96 ± 0.03
24 during the period DoE 0-150.

25 Instead of changing the value of n over time (and therefore those of $\epsilon_K^{2\text{H}}$ and $\epsilon_K^{18\text{o}}$), another
26 possibility is to consider that after some time the relative humidity at the EF (rh_{EF}) was
27 different from 100%, although the EF was still at thermodynamic equilibrium. In that case
28 kinetic effects would have depended on the difference ($rh_{\text{EF}} - rh$) instead of $(1 - rh)$. Figure
29 9b shows the rh_{EF} time course that provided the best model-to-data fit (NSE = 0.92), when
30 $\epsilon_K^{2\text{H}}$ and $\epsilon_K^{18\text{o}}$ were calculated (Eq. (5a-5b-6)). In this second scenario, rh_{EF} decreased from 100

1 to 81 % with a mean value of 99.5 ± 0.03 % for the period DoE 0-150, i.e., in a similar
2 fashion than fitted n values obtained in the 1st scenario. These values were significantly lower
3 than what is calculated with Kelvin's Equation linking rh_{EF} with soil water tension at the EF
4 in the case of liquid-vapor equilibrium, which for the soil retention properties (Merz et al.,
5 2014) would range between 100 and 99.6 %. In a third scenario one could consider a
6 combined decrease of n and rh_{EF} to smaller extents, for which there are no unique solutions at
7 each time step. In any case, only decreasing kinetic effects could provide a better model-to-
8 data fit. In the present study, information on δ^2H and $\delta^{18}O$ of the evaporation flux was missing
9 to address uncertainties in the determination of ϵ_K^{2H} and ϵ_K^{18O} . The experimental setup would
10 also have gained from the addition of appropriate sensors (e.g., micro-psychrometers) to
11 measure the soil surface relative humidity and especially rh_{EF} , although the dimensions of the
12 column would certainly be a limiting factor. Finally note that S_{Ev} calculations using diffusivity
13 ratios determined by Cappa et al. (2003) lead to lower value of S_{Ev} and less good model-to-
14 data fit. A more in depth investigation of the behavior of S_{Ev} (and isotope composition
15 gradients with depth for that matter) with time could be carried out with detailed numerical
16 simulations using an isotope-enabled SVAT model such as SiSPAT-Isotope.

17 **5 Conclusion**

18 Since the initial work of Zimmermann et al. (1967), water stable isotopologues have proven
19 both theoretically and experimentally to be valuable tools for the study of water flow in the
20 soil and at the soil-atmosphere interface. In this work we present the first application of the
21 method of Rothfuss et al. (2013). This study constitutes also the very first long-term
22 application of a—the series of newly developed isotopic monitoring systems—~~novel approach~~
23 based on gas-permeable tubing and isotope-specific infrared laser absorption spectroscopy
24 (Herbstritt et al., 2012; Volkmann and Weiler, 2014)which allows overcoming limitations due
25 to destructive sampling and offline isotope analysis leading to an insufficient time resolution.

26 Our ~~newly developed~~ method proved to be reliable over long time periods and followed
27 quantitatively the progressive isotope enrichment caused by evaporation in an initially
28 saturated soil column. Moreover, it could capture sudden variations following a simulated
29 intense rain event.

30 Simple calculations of isotope compositions' gradients made it possible to evaluate the
31 position of the Evaporation Front and observe how it progressively receded with time in the

1 soil. Confrontation of the model of Craig and Gordon (1965) with data also highlighted
2 uncertainties associated with the determinations of isotope kinetic fractionations and soil
3 relative humidity at the EF when the soil surface dry layer was the most developed and
4 evaporation flux was low.

5 Our method will allow experimentalists to measure and locate the evaporation front in a
6 dynamic and non-destructive manner and to calculate the isotope compositions of the
7 evaporation flux using the model of Craig and Gordon (1965) with much higher time
8 resolution. Provided that the isotope compositions of evapotranspiration and transpiration
9 fluxes are measured or modelled, this method will be especially useful to test hypotheses and
10 improve our understanding of root water uptake processes and the partitioning of
11 evapotranspiration fluxes.

13 **Acknowledgements**

14 This study was conducted in the framework of and with means from the Bioeconomy
15 Portfolio Theme of the Helmholtz Association of German Research Centers. The authors
16 would like to thank Ayhan Egmen and Dieter Mans from the IBG Workshop at
17 Forschungszentrum Jülich for designing and building the acrylic glass column and Holger
18 Wissel for his insight and technical support. Special thanks go to the Institute of Meteorology
19 and Climate Research (IMK-IFU), Karlsruhe Institute of Technology, for providing the water
20 isotopic analyzer for this study.

1 **References**

- 2 Barnes, C. J., and Allison, G. B.: The Distribution of Deuterium and O-18 in Dry Soils .1.
3 Theory, J. Hydrol., 60, 141-156, doi: 10.1016/0022-1694(83)90018-5, 1983.
- 4 Barnes, C. J., and Allison, G. B.: The Distribution of Deuterium and O-18 in Dry Soils .3.
5 Theory for Non-Isothermal Water-Movement, J. Hydrol., 74, 119-135, doi: 10.1016/0022-
6 1694(84)90144-6, 1984.
- 7 [Barnes, C. J., and Allison, G. B.: Tracing of water movement in the unsaturated zone using](#)
8 [stable isotopes of hydrogen and oxygen, J. Hydrol., 100, 143–176, doi:10.1016/0022-](#)
9 [1694\(88\)90184-9, 1988](#)
- 10 Barnes, C. J., and Walker, G. R.: The Distribution of Deuterium and O-18 during Unsteady
11 Evaporation from a Dry Soil, J. Hydrol., 112, 55-67, doi: 10.1016/0022-1694(89)90180-7,
12 1989.
- 13 Blasch, K. W., and Bryson, J. R.: Distinguishing sources of ground water recharge by using
14 delta H-2 and delta O-18, Ground Water, 45, 294-308, doi: 10.1111/j.1745-
15 6584.2006.00289.x, 2007.
- 16 Braud, I., Bariac, T., Gaudet, J. P., and Vauclin, M.: SiSPAT-Isotope, a coupled heat, water
17 and stable isotope (HDO and (H₂O)-O-18) transport model for bare soil. Part I. Model
18 description and first verifications, J. Hydrol., 309, 277-300, doi:
19 10.1016/j.jhydrol.2004.12.013, 2005.
- 20 [Braud, I., Biron, P., Bariac, T., Richard, P., Canale, L., Gaudet, J. P., and Vauclin, M.:](#)
21 [Isotopic composition of bare soil evaporated water vapor. Part I: RUBIC IV experimental](#)
22 [setup and results, J. Hydrol., 369, 1-16, DOI 10.1016/j.jhydrol.2009.01.034, 2009a.](#)
- 23 [Braud, I., Bariac, T., Biron, P., and Vauclin, M.: Isotopic composition of bare soil evaporated](#)
24 [water vapor. Part II: Modeling of RUBIC IV experimental results, J. Hydrol., 369, 17-29,](#)
25 [DOI 10.1016/j.jhydrol.2009.01.038, 2009b.](#)
- 26 [Brunel, J. P., Walker, G. R, and Kennetsmith, A. K.: Field Validation of Isotopic Procedures](#)
27 [for Determining Sources of Water Used by Plants in a Semiarid Environment, J. Hydrol., 167,](#)
28 [351-368, doi: 10.1016/0022-1694\(94\)02575-V, 1995.](#)

1 [Brutsaert, W.: A theory for local evaporation \(or heat transfer\) from rough and smooth](#)
2 [surfaces at ground level, Water Resour. Res., 11, 543-550, doi: 10.1029/WR011i004p00543,](#)
3 [1975.](#)

4 Craig, H.: Isotopic Variations in Meteoric Waters, Science, 133, 1702-~~&~~-1703, doi:
5 10.1126/science.133.3465.1702, 1961.

6 Craig, H., and Gordon, L. I.: Deuterium and oxygen 18 variations in the ocean and marine
7 atmosphere, Stable Isotopes in Oceanographic Studies and Paleotemperatures, Spoleto, Italy,
8 1965, 9-130, 1965.

9 [DePaolo, D. J., Conrad, M. E., Maher, K., and Gee, G. W.: Evaporation effects on oxygen and](#)
10 [hydrogen isotopes in deep vadose zone pore fluids at Hanford, Washington, Vad. Zone. J., 3,](#)
11 [220-232, doi:10.2113/3.1.220, 2004.](#)

12 [Dongmann, G., H. W. Nurnberg, H. Forstel, and Wagener, K.: Enrichment of H₂¹⁸O in](#)
13 [Leaves of Transpiring Plants, Radiat Environ Bioph, 1, 41-52, doi: 10.1007/Bf01323099,](#)
14 [1974.](#)

15 Dubbert, M., Cuntz, M., Piayda, A., Maguás, C., and Werner, C.: Partitioning
16 evapotranspiration – Testing the Craig and Gordon model with field measurements of oxygen
17 isotope ratios of evaporative fluxes, J. Hydrol., 496, 142-153, doi:
18 10.1016/j.jhydrol.2013.05.033, 2013.

19 [Gaj, M., Beyer, M., Koeniger, P., Wanke, H., Hamutoko, J., and Himmelsbach, T.: In-situ](#)
20 [unsaturated zone stable water isotope \(²H and ¹⁸O\) measurements in semi-arid environments](#)
21 [using tunable off-axis integrated cavity output spectroscopy, Hydrol. Earth Syst. Sci. Discuss.](#)
22 [12, 6115-6149, doi:10.5194/hessd-12-6115-2015, 2015.](#)

23 [Gat, J.: Comments on the Stable Isotope Method in Regional Groundwater Investigations,](#)
24 [Water Resour. Res., 7, 980-993, doi: 10.1029/WR007i004p00980, 1971](#)

25 [Goldsmith, G.R., Munoz-Villers, L.E., Holwerda, F., McDonnell, J.J., Asbjornsen, H.,](#)
26 [Dawson, T.E.: Stable isotopes reveal linkages among ecohydrological processes in a](#)
27 [seasonally dry tropical montane cloud forest, Ecohydrology, 5, 779-790, doi:](#)
28 [10.1002/eco.268, 2011.](#)

29 Gonfiantini, R.: Standards for stable isotope measurements in natural compounds, Nature,
30 271, 534-536, doi: 10.1038/271534a0, 1978.

- 1 Haverd, V., and Cuntz, M.: Soil-Litter-Iso: A one-dimensional model for coupled transport of
2 heat, water and stable isotopes in soil with a litter layer and root extraction, *J. Hydrol.*, 388,
3 438-455, doi: 10.1016/j.jhydrol.2010.05.029, 2010.
- 4 Herbstritt, B., Gralher, B., and Weiler, M.: Continuous in situ measurements of stable
5 isotopes in liquid water, *Water Resour. Res.*, 48, doi: 10.1029/2011wr011369, 2012.
- 6 Hu, Z. M., Wen, X. F., Sun, X. M., Li, L. H., Yu, G. R., Lee, X. H., and Li, S. G.: Partitioning
7 of evapotranspiration through oxygen isotopic measurements of water pools and fluxes in a
8 temperate grassland, *J Geophys Res-Biogeo*, 119, 358-371, ~~Doi~~ doi: 10.1002/2013jg002367,
9 2014.
- 10 Jasechko, S., Sharp, Z. D., Gibson, J. J., Birks, S. J., Yi, Y., and Fawcett, P. J.: Terrestrial
11 water fluxes dominated by transpiration, *Nature*, 496, 347-~~351~~, doi: 10.1038/Nature11983,
12 2013.
- 13 [Litaor, M.I.: Review of Soil Solution Samplers. *Water Resour. Res.*, 24, 727-733, doi:](#)
14 [10.1029/Wr024i005p00727, 1988](#)
- 15
- 16 Liu, Z. F., Bowen, G. J., and Welker, J. M.: Atmospheric circulation is reflected in
17 precipitation isotope gradients over the conterminous United States, *J. Geophys. Res.-Atmos.*,
18 115, doi: 10.1029/2010jd014175, 2010.
- 19 [Merlivat, L.: Molecular Diffusivities of H₂¹⁶O, HD¹⁶O, and H₂¹⁸O in Gases, *J. Chem.*](#)
20 [Phys., doi: 10.1063/1.436884, 1978](#)
- 21 [Merlivat, L., and Coantic, M.: Study of Mass-Transfer at Air-Water-Interface by an Isotopic](#)
22 [Method, *J. Geophys. Res.-Oc. Atm.*, 80, 3455-3464, doi: 10.1029/Jc080i024p03455, 1975](#)
- 23 [Majoube, M.: Oxygen-18 and Deuterium Fractionation between Water and Steam, *J. Chim.*](#)
24 [Phys. Phys.-Chim. Biol., 68, 1423-1436, 1971.](#)
- 25 [Mathieu, R., and Bariac, T.: A numerical model for the simulation of stable isotope profiles in](#)
26 [drying soils, 101, 12685–12696, *J. Geophys. Res.-Atmos.*, doi: 10.1029/96jd00223, 1996](#)
- 27

1 Merz, S., Pohlmeier, A., Vanderborcht, J., van Dusschoten, D., and Vereecken, H.: Moisture
2 profiles of the upper soil layer during evaporation monitored by NMR, *Water Resour. Res.*,
3 50, 5184-5195, ~~Doi~~doi: 10.1002/2013wr014809, 2014.

4 Murray, F. W.: On the Computation of Saturation Vapor Pressure, *J. Appl. Meteorol.*, 6, 203-
5 204, doi: 10.1175/1520-0450, 1967.

6 Nash, J. E., and Sutcliffe, J. V.: River flow forecasting through conceptual models part I -A
7 discussion of principles, *Journal of Hydrology*, 10, 282-290, doi:10.1016/0022-
8 1694(70)90255-6, 1970

9 Oerter, E., Finstad, K., Schaefer, J., Goldsmith, G. R., Dawson, T., and Amundson, R.:
10 Oxygen isotope fractionation effects in soil water via interaction with cations (Mg, Ca, K, Na)
11 adsorbed to phyllosilicate clay minerals, *J. Hydrol.*, 515, 1-9, doi:
12 10.1016/j.jhydrol.2014.04.029, 2014.

13 Peng, T. R., Lu, W. C., Chen, K. Y., Zhan, W. J., and Liu, T. K.: Groundwater-recharge
14 connectivity between a hills-and-plains' area of western Taiwan using water isotopes and
15 electrical conductivity, *J. Hydrol.*, 517, 226-235, ~~DOI~~doi: 10.1016/j.jhydrol.2014.05.010,
16 2014.

17 Phillips, D. L., and Gregg, J. W.: Uncertainty in source partitioning using stable isotopes,
18 *Oecologia*, 127, 171-179, doi: 10.1007/s004420000578, 2001.

19 Rothfuss, Y., Biron, P., Braud, I., Canale, L., Durand, J. L., Gaudet, J. P., Richard, P.,
20 Vauclin, M., and Bariac, T.: Partitioning evapotranspiration fluxes into soil evaporation and
21 plant transpiration using water stable isotopes under controlled conditions, *Hydrol. Process.*,
22 24, 3177-3194, doi: 10.1002/Hyp.7743, 2010.

23 Rothfuss, Y., Braud, I., Le Moine, N., Biron, P., Durand, J. L., Vauclin, M., and Bariac, T.:
24 Factors controlling the isotopic partitioning between soil evaporation and plant transpiration:
25 Assessment using a multi-objective calibration of SiSPAT-Isotope under controlled
26 conditions, *J. Hydrol.*, 442, 75-88, doi: 10.1016/j.jhydrol.2012.03.041, 2012.

27 Rothfuss, Y., Vereecken, H., and Brüggemann, N.: Monitoring water stable isotopic
28 composition in soils using gas-permeable tubing and infrared laser absorption spectroscopy,
29 *Water Resour. Res.*, 49, 1-9, doi: 10.1002/wrcr.20311, 2013.

1 Schmidt, M., Maseyk, K., Lett, C., Biron, P., Richard, P., Bariac, T., and Seibt, U.:
2 Concentration effects on laser-based d18O and d2H measurements and implications for the
3 calibration of vapour measurements with liquid standards, *Rapid Commun. Mass Spectrom.*,
4 24, 3553–3561, doi: 10.1002/rcm.4813, 2010.

5 Shahraeeni, E., Lehmann, P., and Or, D.: Coupling of evaporative fluxes from drying porous
6 surfaces with air boundary layer: Characteristics of evaporation from discrete pores, *Water*
7 | *Resour. Res.*, 48, ~~Doi~~-doi: 10.1029/2012wr011857, 2012.

8 Singleton, M. J., Sonnenthal, E. L., Conrad, M. E., DePaolo, D. J., and Gee, G. W.:
9 Multiphase reactive transport modeling of seasonal infiltration events and stable isotope
10 fractionation in unsaturated zone pore water and vapor at the Hanford site, *Vadose Zone J.*, 3,
11 | 775-785, doi: 10.2113/3.3.775, 2004.

12 Sofer, Z., and Gat, J. R.: Activities and Concentrations of O-18 in Concentrated Aqueous Salt
13 Solutions - Analytical and Geophysical Implications, *Earth Planet. Sc. Lett.*, 15, 232-&, doi:
14 10.1016/0012-821x(72)90168-9, 1972.

15 Stingaciu, L. R., Pohlmeier, A., Blumler, P., Weihermuller, L., van Dusschoten, D., Stapf, S.,
16 and Vereecken, H.: Characterization of unsaturated porous media by high-field and low-field
17 NMR relaxometry, *Water Resour. Res.*, 45, doi: 10.1029/2008wr007459, 2009.

18 Sutanto, S. J., Wenninger, J., Coenders-Gerrits, A. M. J., and Uhlenbrook, S.: Partitioning of
19 evaporation into transpiration, soil evaporation and interception: a comparison between
20 isotope measurements and a HYDRUS-1D model, *Hydrol. Earth Syst. Sc.*, 16, 2605-2616,
21 doi: 10.5194/hess-16-2605-2012, 2012.

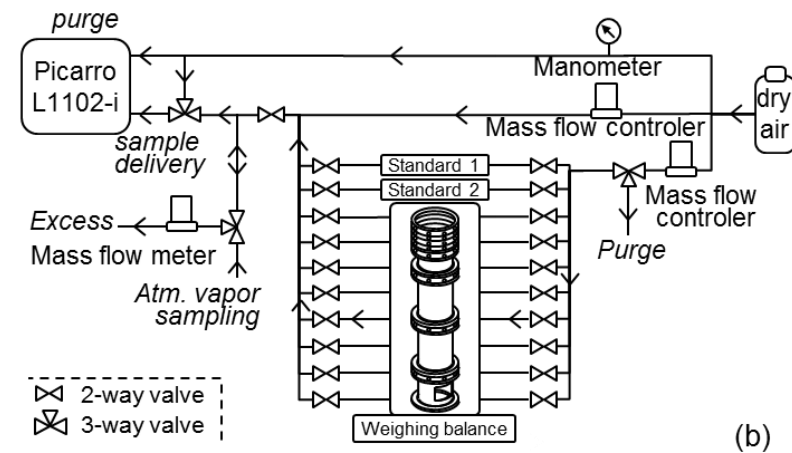
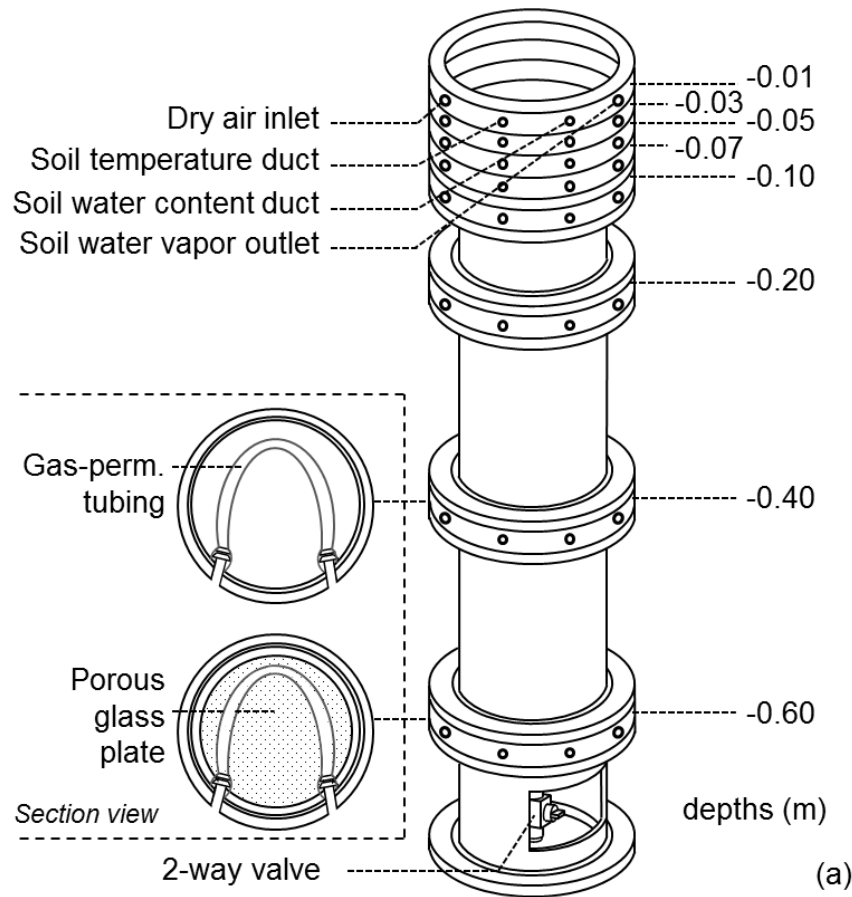
22 Volkmann, T. H. M., and Weiler, M.: Continual in situ monitoring of pore water stable
23 isotopes in the subsurface, *Hydrol. Earth Syst. Sc.*, 18, 1819-1833, doi: 10.5194/hess-18-
24 1819-2014, 2014.

25 Wang, P., Song, X. F., Han, D. M., Zhang, Y. H., and Liu, X.: A study of root water uptake of
26 crops indicated by hydrogen and oxygen stable isotopes: A case in Shanxi Province, China,
27 *Agric. Water Manage.*, 97, 475-482, doi: 10.1016/j.agwat.2009.11.008, 2010.

28 Yopez, E. A., Huxman, T. E., Ignace, D. D., English, N. B., Weltzin, J. F., Castellanos, A. E.,
29 and Williams, D. G.: Dynamics of transpiration and evaporation following a moisture pulse in
30 semiarid grassland: A chamber-based isotope method for partitioning flux components, *Agr.*
31 *Forest Meteorol.*, 132, 359-376, doi: 10.1016/j.agrformet.2005.09.006, 2005.

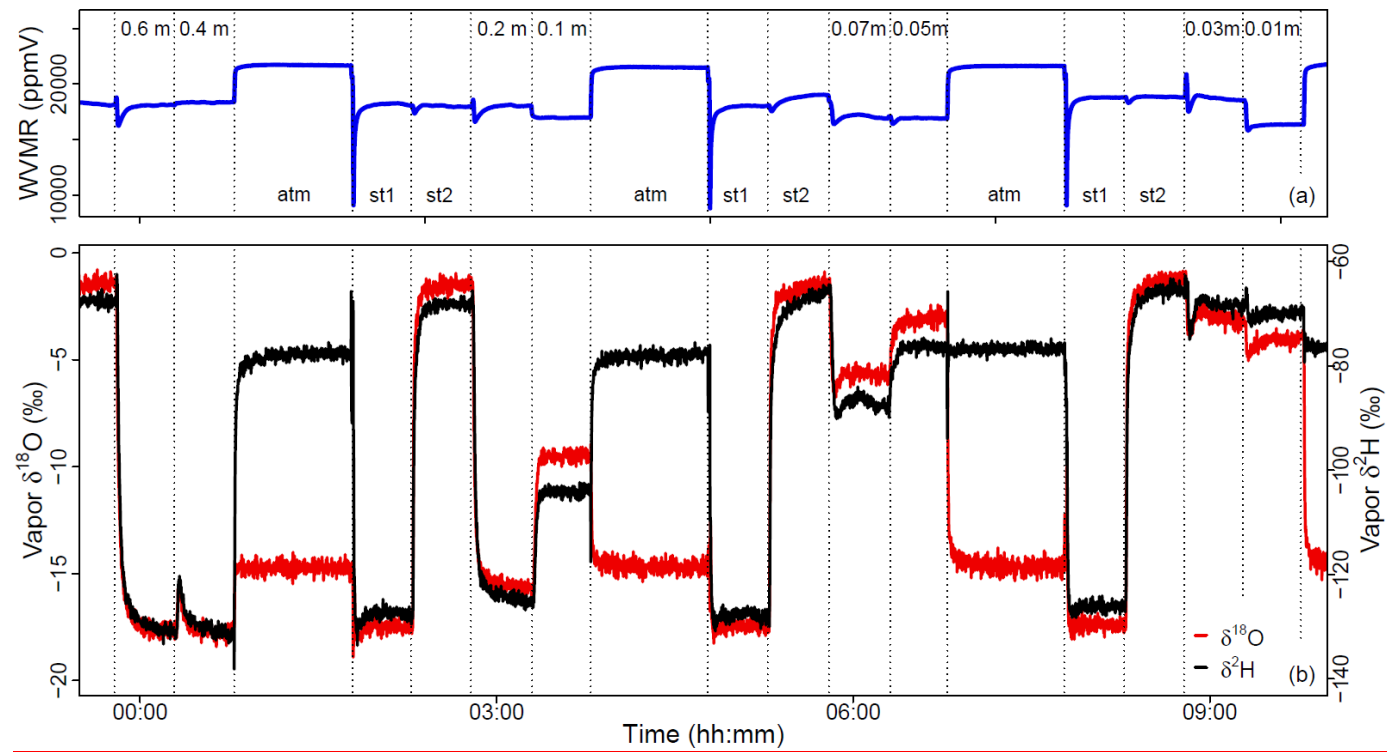
- 1 Zimmermann, U., Ehhalt, D., and Münnich, K. O.: Soil water movement and
- 2 evapotranspiration: changes in the isotopic composition of the water, Symposium of Isotopes
- 3 in Hydrology, Vienna, 1967, 567–584.

1 **Figures**

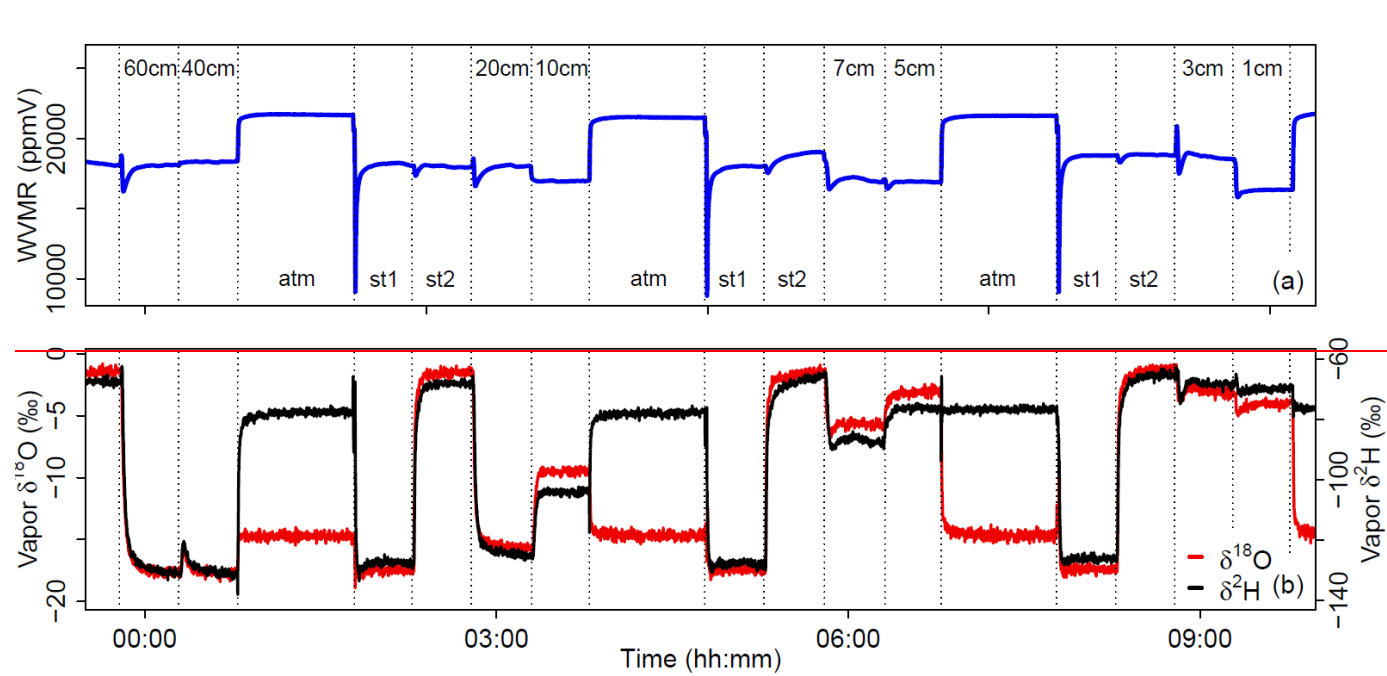


2

3 Figure 1. (a) Scheme of the acrylic glass column used in the experiment; (b) experimental setup for sampling water vapor at the different soil
 4 depths of the soil column, from the ambient air, and from the two soil water standards (standard 1 and 2).
 5



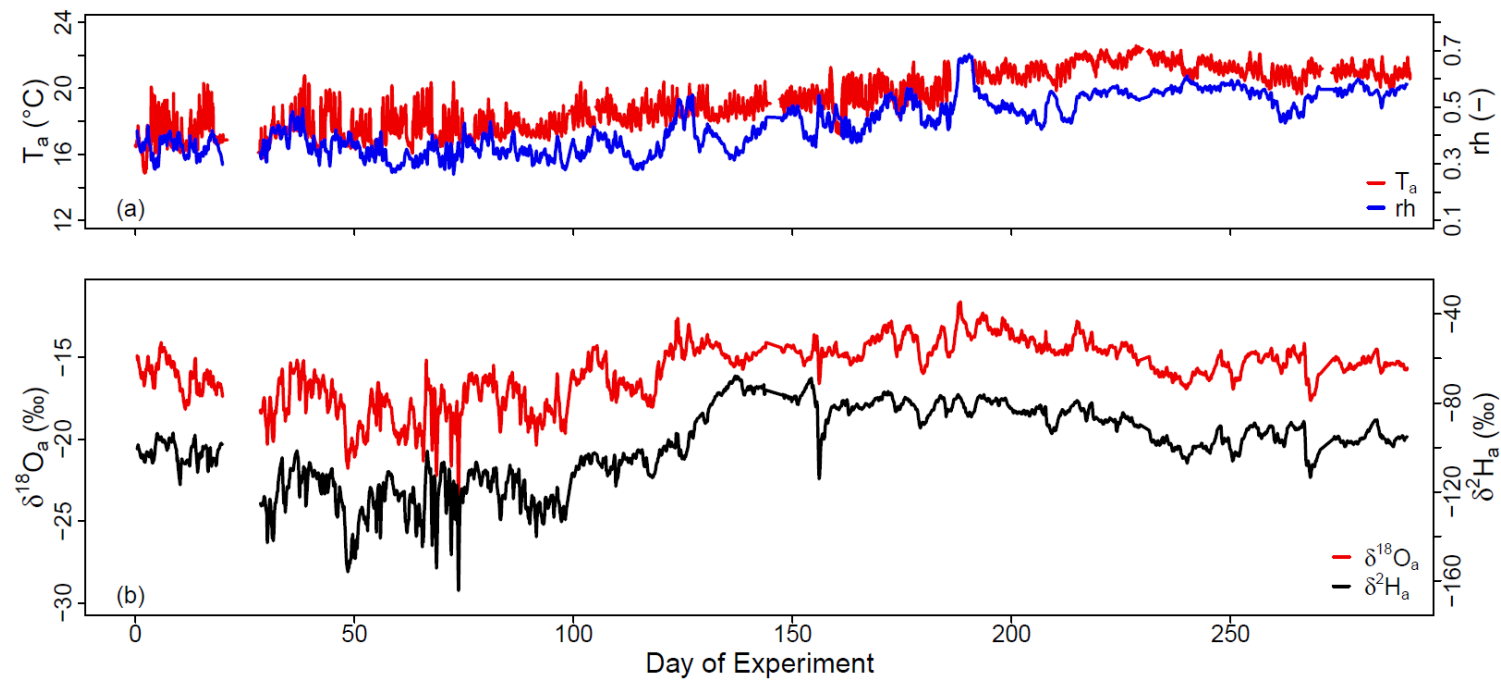
1



1

2 Figure 2. Water vapor mixing ratio (*WVMR*, in ppmv) and isotope composition ($\delta^{18}\text{O}$ and $\delta^2\text{H}$, in ‰ V-SMOW) of the water vapor sampled
 3 on Day of Experiment 150 from the ambient air (“atm”), both standards (“st1” and “st2”), and from the tubing sections at soil depths 1, 3, 5, 7,
 4 10, 20, 40, and 60 cm.

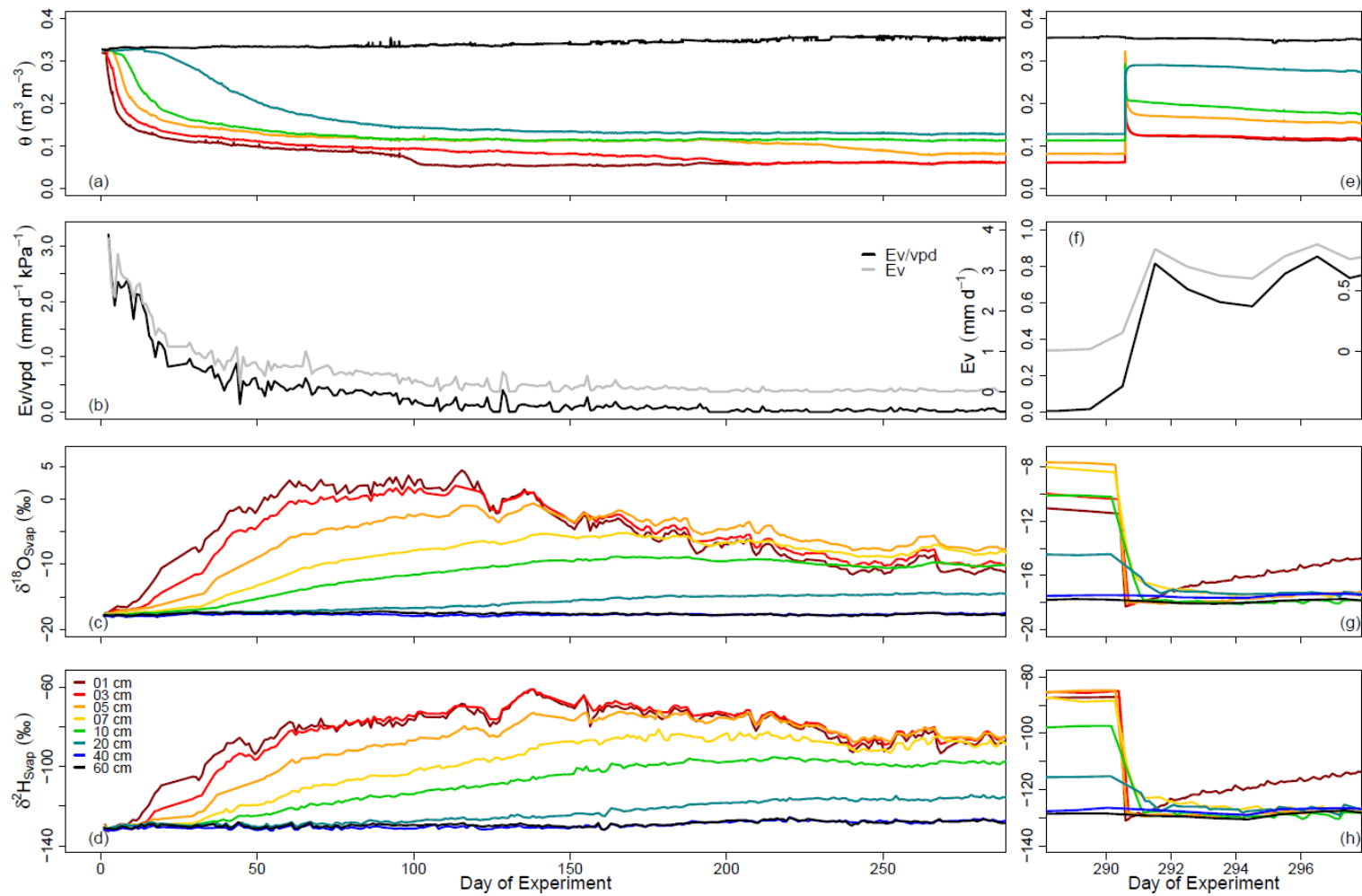
5



1

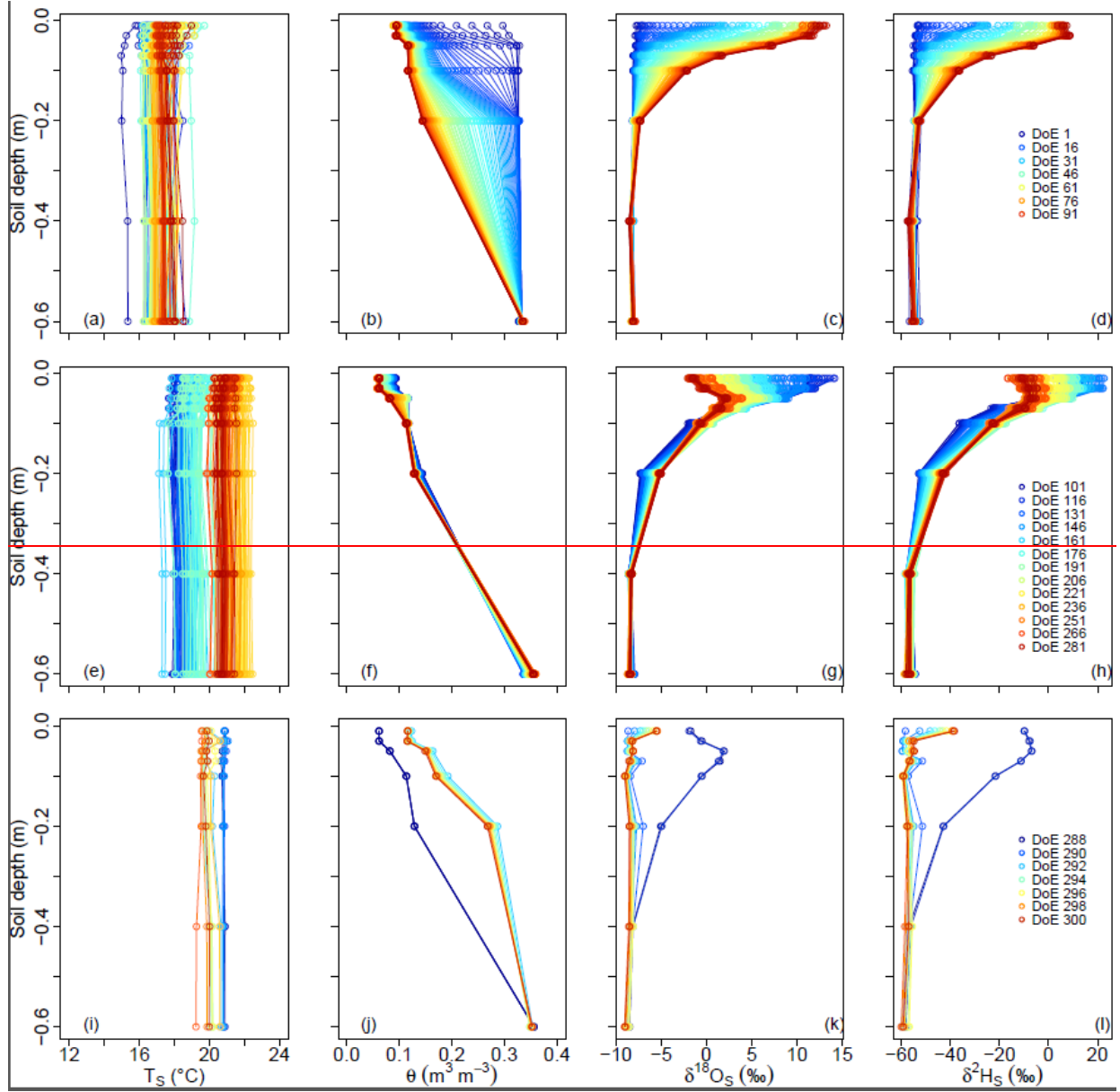
2 Figure 3. Time series of the laboratory ambient air temperature (T_a , in $^{\circ}\text{C}$), relative humidity (rh , in %) and water vapor isotope compositions
 3 | ($\delta^{18}\text{O}_a$ and $\delta^2\text{H}_a$, in ‰ V-SMOW) over the course of the experiment.-

4

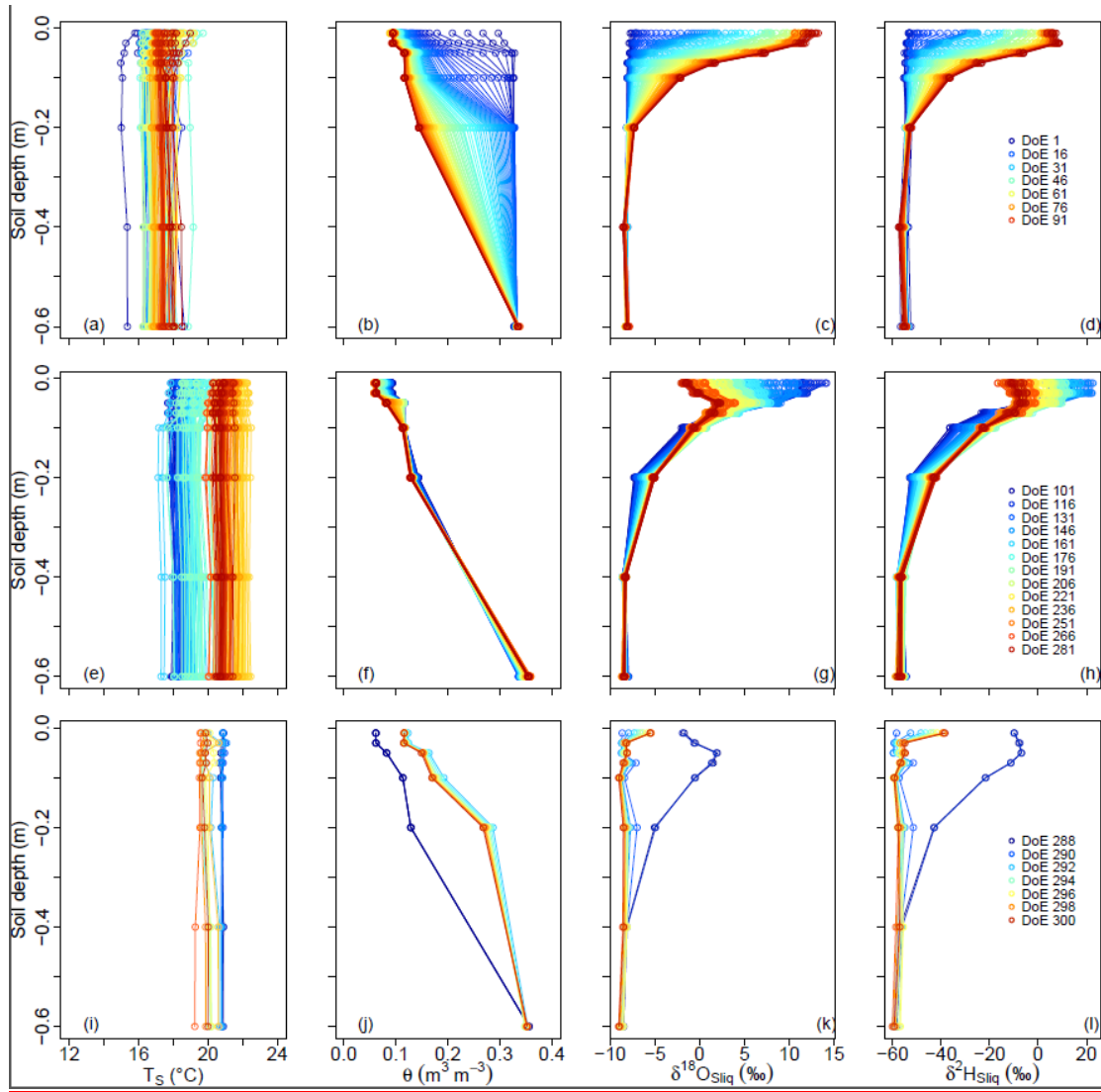


1

2 Figure 4. Time series of soil temperature (T_s , in $^{\circ}\text{C}$), of water content (θ , in $\text{m}^3 \text{m}^{-3}$), of
 3 evaporation flux (Ev , in mm d^{-1}), and water vapor isotope compositions ($\delta^{18}\text{O}_{\text{svap}}$ and $\delta^2\text{H}_{\text{svap}}$, in ‰ V-SMOW) during the course of the experiment.

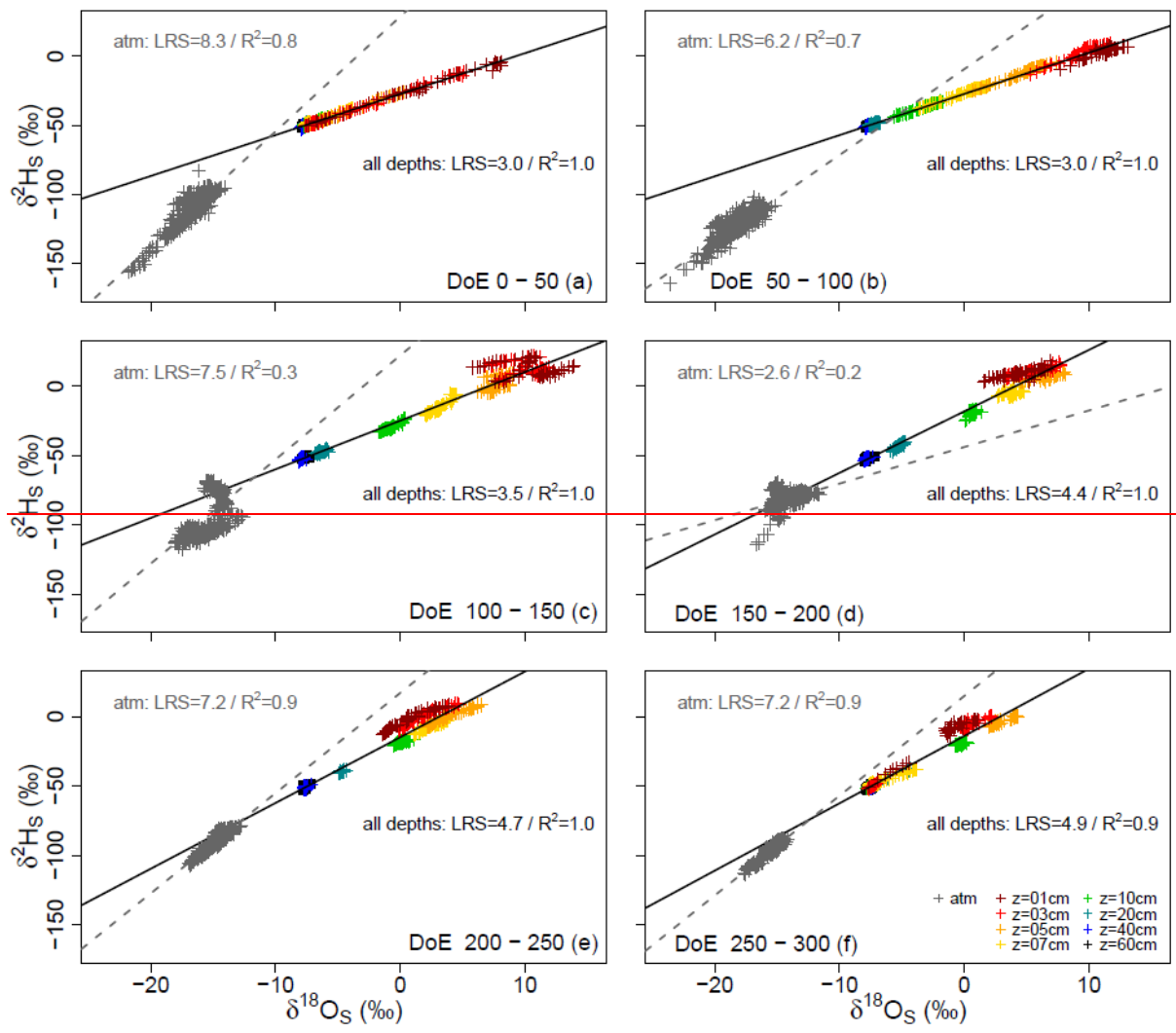


1

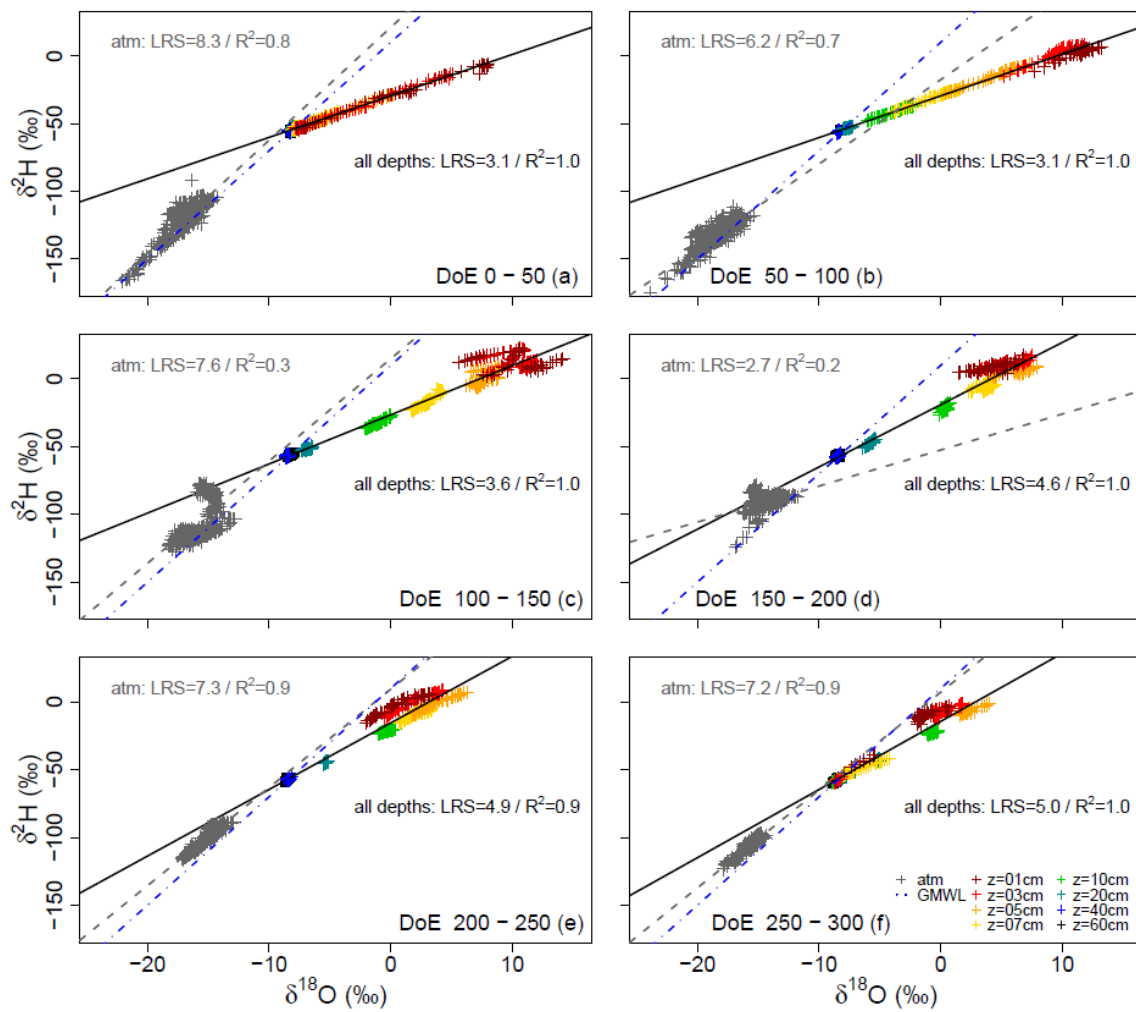


1

2 Figure 5. Soil temperature (T_S , in $^{\circ}\text{C}$), water content (θ , in $\text{m}^3 \text{m}^{-3}$), and liquid water isotope
 3 | compositions ($\delta^{18}\text{O}_{\text{Sliq}}$ and $\delta^2\text{H}_{\text{Sliq}}$, in ‰ V-SMOW) profiles from Day of Experiment (DoE) 0
 4 | - 100 (top panel), from DoE 101 - 287 (middle panel), and from DoE 288 - 299 (bottom
 5 | panel).
 6

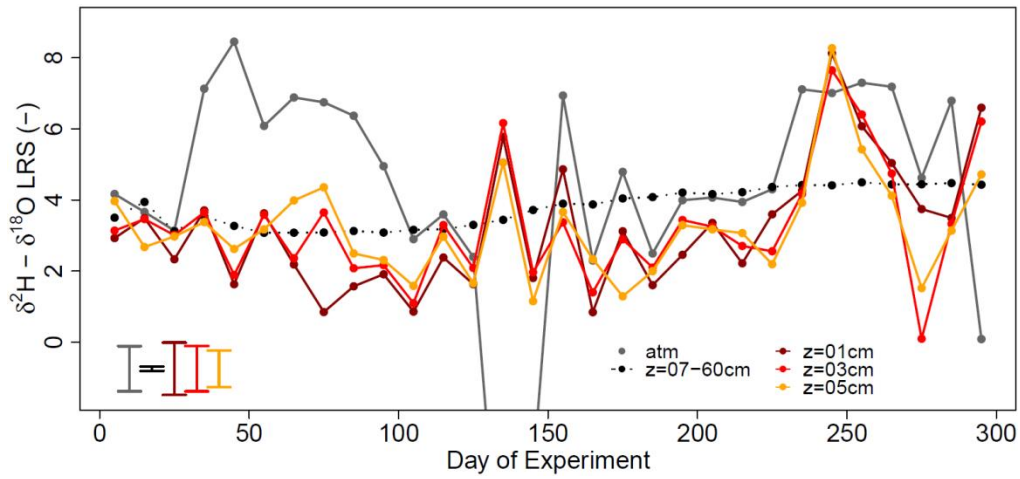


1



1
 2 Figure 6. Linear regressions (gray dotted line) between laboratory atmosphere water vapor
 3 $\delta^{18}\text{O}$ and $\delta^2\text{H}$ (in ‰ V-SMOW) and between soil water $\delta^{18}\text{O}$ and $\delta^2\text{H}$ (solid black line). Each
 4 plot represents data from 50 consecutive days of experiment (DoE). Global Meteoric Water
 5 Line (GMWL, define by $\delta^2\text{H} = 8 * \delta^{18}\text{O} + 10$, in blue dotted line) is shown on each sub-plot for
 6 comparison. Coefficient of ~~correlation-determination~~ (R^2) as well as the slope of the linear
 7 regressions (LRS) are reported-

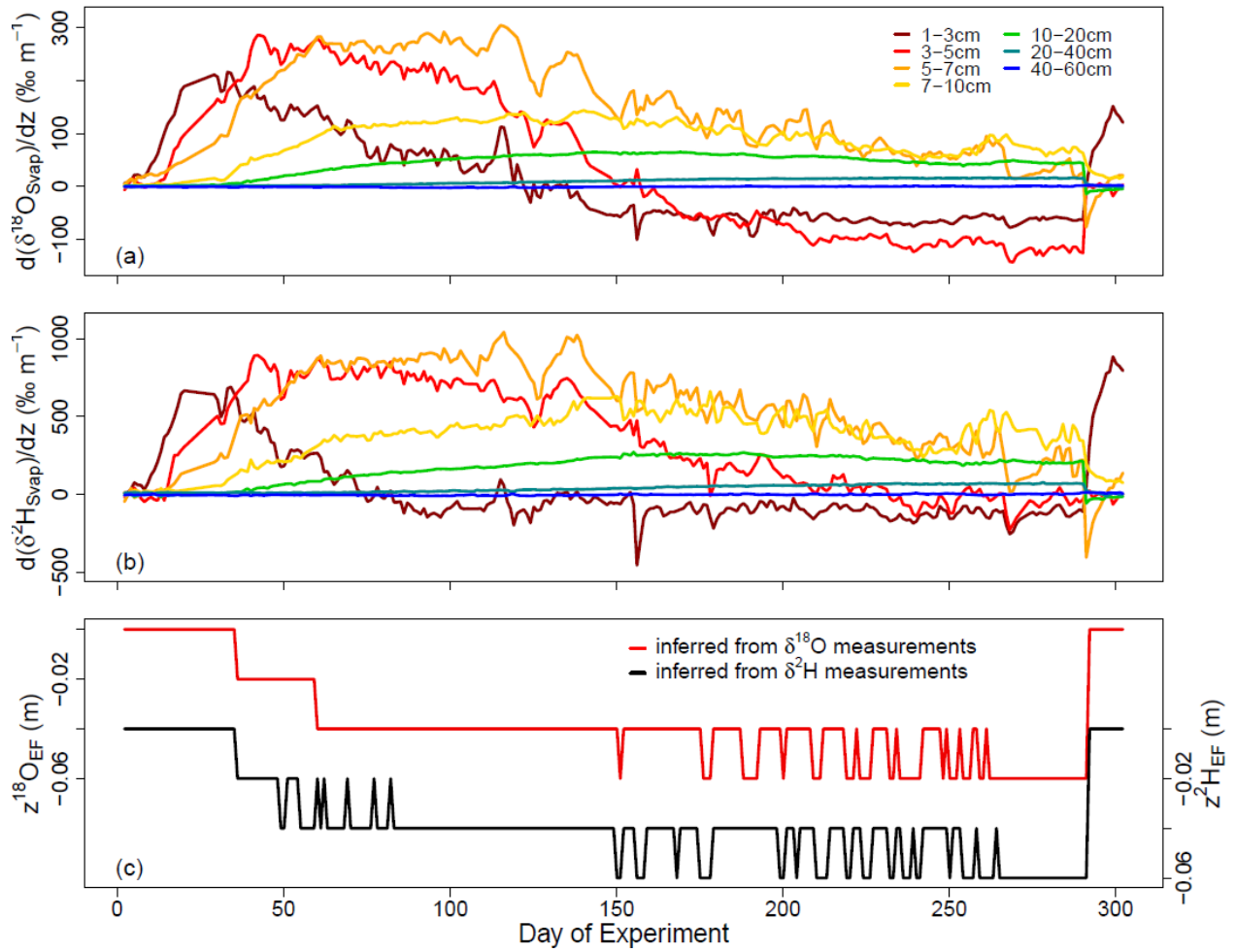
8



1

2 Figure 7. Time course of the slopes of the $\delta^{18}\text{O}$ - $\delta^2\text{H}$ linear regressions (LRS) for time
 3 intervals of ten consecutive days of atmosphere data (gray solid line), soil data from the upper
 4 three layers (01, 03, and 05 cm, colored solid lines), and combined soil data from the
 5 remaining bottom layers (from 07 to 60 cm, black dotted line). Mean standard errors are
 6 represented by the error bars in the bottom left corner.

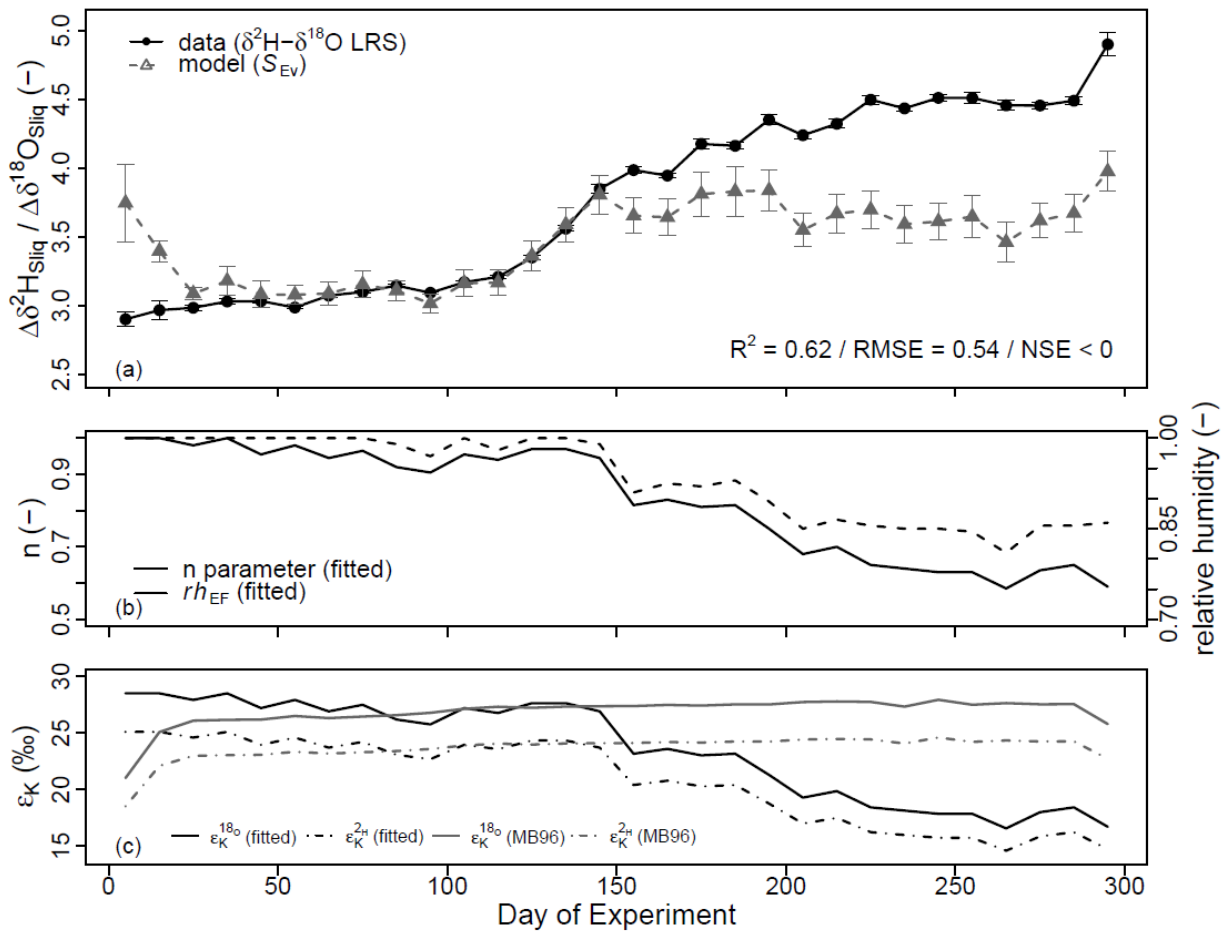
7



1

2 Figure 8. (a) and (b) $^1\text{H}^2\text{H}^{16}\text{O}$ and $^1\text{H}_2^{18}\text{O}$ composition gradients calculated between
 3 consecutive observation points in the soil. (c) Evolution of the evaporation front depths $z^{18}\text{O}_{\text{EF}}$
 4 (red solid line) and $z^2\text{H}_{\text{EF}}$ (black solid line) inferred from the $^1\text{H}^2\text{H}^{16}\text{O}$ and $^1\text{H}_2^{18}\text{O}$
 5 composition gradients

6



1
2 Figure 9. (a) Comparison between soil liquid water $\delta^{18}\text{O}-\delta^2\text{H}$ linear regressions slopes (LRS,
3 solid black line) calculated for time intervals of ten consecutive days and simulated time
4 series of evaporation line slope (S_{Ev} , dotted gray line) obtained from Equations (3-6) (Gat et
5 al., 1971, Merlivat, 1978, Mathieu and Bariac, 1996). Black error bars give the standard errors
6 of the estimated $\delta^{18}\text{O}-\delta^2\text{H}$ LRS. Gray error bars are the standard errors associated with
7 calculation of S_{Ev} following Phillips and Gregg (2001). Coefficient of determination (R^2),
8 Root Mean Square Error (RMSE) and Nash and Sutcliffe Efficiency (NSE) between model
9 and data are reported. (b) Time series of n parameter (Eq. (6)) and soil relative humidity at the
10 Evaporation Front (rh_{EF}) that provided the best model-to-data fit. (c) $\epsilon_K^{2\text{H}}$ and $\epsilon_K^{18\text{O}}$ time series
11 obtained from fitted n values ("fitted") and calculated following Mathieu and Bariac (1996)
12 ("MB96")